(2)

NAVAL POSTGRADUATE SCHOOL
Monterey, California

THESIS

PERFORMANCE OF DIRECT BIT DETECTION
RECEIVERS FOR MULTIPLE LEVEL
PHASE-SHIFT-KEYED MODULATION

by

Tan, Chee Seng

June 1986

Thesis Advisor: D. Bukofzer

Approved for public release; distribution is unlimited

SECURITY CLASSIFICATION OF THIS PAGE

AD-A178564

REPORT DOCUMENTATION PAGE

1a. REPORT SECURITY CLASSIFICATION UNCLASSIFIED	1b. RESTRICTIVE MARKINGS
2a. SECURITY CLASSIFICATION AUTHORITY	3. DISTRIBUTION / AVAILABILITY OF REPORT Approved for public release; distribution is unlimited
2b. DECLASSIFICATION / DOWNGRADING SCHEDULE	
4. PERFORMING ORGANIZATION REPORT NUMBER(S)	5. MONITORING ORGANIZATION REPORT NUMBER(S)
6a. NAME OF PERFORMING ORGANIZATION Naval Postgraduate School 6b. OFFICE SYMBOL (If applicable) 62	7a. NAME OF MONITORING ORGANIZATION Naval Postgraduate School
6c. ADDRESS (City, State, and ZIP Code) Monterey, California 93943-5000	7b. ADDRESS (City, State, and ZIP Code) Monterey, California 93943-5000
8a. NAME OF FUNDING / SPONSORING ORGANIZATION 8b. OFFICE SYMBOL (If applicable)	9. PROCUREMENT INSTRUMENT IDENTIFICATION NUMBER
8c. ADDRESS (City, State, and ZIP Code)	10. SOURCE OF FUNDING NUMBERS PROGRAM ELEMENT NO. / PROJECT NO. / TASK NO / WORK UNIT ACCESSION NO.

11. TITLE (Include Security Classification)
PERFORMANCE OF DIRECT BIT DETECTION RECEIVERS FOR MULTIPLE LEVEL PHASE-SHIFT-KEYED MODULATION

12. PERSONAL AUTHOR(S)
Tan, Chee Seng

13a. TYPE OF REPORT	13b. TIME COVERED	14. DATE OF REPORT (Year, Month, Day)	15. PAGE COUNT
Master's Thesis	FROM _____ TO _____	86 June 20	80

16. SUPPLEMENTARY NOTATION

17. COSATI CODES			18. SUBJECT TERMS (Continue on reverse if necessary and identify by block number)
FIELD	GROUP	SUB-GROUP	Digital Communications; M-ary PSK; Direct Bit Detection

19. ABSTRACT (Continue on reverse if necessary and identify by block number)

A new receiver algorithm for M-ary Phase-Shift-Keyed modulation is proposed which provides for direct bit detection (DBD) instead of the traditional approach of symbol detection followed by bit regeneration. DBD eliminates the intermediate step of symbol detection and bit regeneration, reduces the amount of computation, allows for binary rather than M-ary decisions, and permits parallel regeneration of bits. All these factors provide an attractive scheme for high speed digital implementation. Receiver structures for DBD of 8-PSK and 16-PSK signals are proposed and the resulting bit error rates (BER) analyzed for transmission over an additive white Gaussian noise channel. In both cases, receiver structures are developed which provide no loss in BER performance when compared to that of conventional phase detection receivers. The proposed receivers' performance was analyzed

20. DISTRIBUTION / AVAILABILITY OF ABSTRACT ☒ UNCLASSIFIED/UNLIMITED ☐ SAME AS RPT ☐ DTIC USERS	21. ABSTRACT SECURITY CLASSIFICATION UNCLASSIFIED
22a. NAME OF RESPONSIBLE INDIVIDUAL Prof D. Bukofzer	22b. TELEPHONE (Include Area Code) (408)646-2859 22c. OFFICE SYMBOL 62Bh

DD FORM 1473, 84 MAR 83 APR edition may be used until exhausted
All other editions are obsolete

SECURITY CLASSIFICATION OF THIS PAGE

alongside channel coding techniques. Coding gains of 2.5-5 dB at a BER of 10^{-5} were shown to be feasible with simple block or convolutional codes.

Approved for public release; distribution is unlimited.

Performance of Direct Bit Detection Receivers for Multiple Level Phase-Shift-Keyed Modulation

by

Tan, Chee Seng
Civilian, Ministry of Defence, Singapore
B.A., Engineering Science, Oxford University, 1980

Submitted in partial fulfillment of the requirements for the degree of

MASTER OF SCIENCE IN ELECTRICAL ENGINEERING

from the

NAVAL POSTGRADUATE SCHOOL
June 1986

Author: _____
Tan, Chee Seng

Approved by: _____
Daniel Bukofzer, Thesis Advisor

_____
Jeffrey B. Knorr, Second Reader

_____
Harriett B. Rigas, Chairman, Department of Electrical and Computer Engineering

_____
John N. Dyer,
Dean of Science and Engineering

ABSTRACT

A new receiver algorithm for M-ary Phase-Shift-Keyed modulation is proposed which provides for direct bit detection (DBD) instead of the traditional approach of symbol detection followed by bit regeneration. DBD eliminates the intermediate step of symbol detection and bit regeneration, reduces the amount of computation, allows for binary rather than M-ary decisions; and permits parallel regeneration of bits. All these factors provide an attractive scheme for high speed digital implementation. Receiver structures for DBD of 8-PSK and 16-PSK signals are proposed and the resulting bit error rates (BER) analyzed for transmission over an additive white Gaussian noise channel. In both cases, receiver structures are developed which provide no loss in BER performance when compared to that of conventional phase detection receivers. The proposed receivers' performance was analyzed alongside channel coding techniques. Coding gains of 2.5-5 dB at a BER of 10^{-5} were shown to be feasible with simple block or convolutional codes.

TABLE OF CONTENTS

LIST OF FIGURES

LIST OF TABLES

I. INTRODUCTION

Information sources can be classified into two categories based on the nature of their outputs, namely analog information and discrete information sources. Analog information sources such as a microphone actuated by speech, or a TV camera scanning a scene, emit one or more continuous amplitude signals. These analog information sources can be transformed into discrete information sources through the process of sampling and quantizing in order to allow transmission through a digital communication channel. Discrete information sources such as a teletype machine or a computer producing an alphanumeric output generate a sequence of discrete source symbols and therefore need no further digitizing.

The discrete outputs of the information sources are converted through a source encoder into a binary sequence of 0's and 1's by assigning codewords to the symbols in its input sequence. The modulator in the system then accepts these bit streams as its input and converts the bits stream into electrical waveforms suitable for transmission over the communication channel. The modulator can assign waveforms to a group of bits of arbitrary size. For example, in a 4-bit group size, the modulator needs to assign sixteen distinct waveforms to represent the sixteen different combinations of 4-binary bits and this is known as a 16-state modulation. In general, non-binary modulation techniques are simply referred to as M-ary modulation.

At present, binary and 4-ary modulation techniques are the more common methods utilized and implemented. However, with the crowded conditions prevailing in many regions of the radio spectrum and the emphasis on modern digital satellite transmission techniques, there is a need for achieving

improved spectrum utilization. The higher order M-ary (M=8 and above) modulation techniques which tend to be spectrally more efficient than the binary or 4-ary modulations at the expense of signal-to-noise ratio and are now employed more frequently. With new developments in the more efficient high-power microwave amplifier designs and advancements in solid-state technology, it is probable that future generations of communication system will be able to operate at low signal-to-noise ratios so as to enable the use of the more spectrally efficient modulation techniques.

Since digital information transmission is based on carriers modulated by the symbol waveforms, the symbol error probabilities can often be computed directly. As a result, the derivation of symbol error probabilities can be found in many references (see [Ref. 1: pp. 228-234, Ref. 2: pp. 204-207] for examples). However, from the viewpoint of a binary digital communication system, the bit error rate is often a better performance criteria and offers a more uniform measure when comparing performances of systems with different levels of modulation. As the bit error probabilities for M-ary modulation systems are not found in references, the first part of this thesis was devoted to developing a general receiver structure for M-ary PSK modulation and deriving a general relation between bit and symbol error probabilities. Receivers for direct bit detection applicable to 8-ary and 16-ary PSK modulations were proposed next, and the bit error rate computed and compared to that of a standard phase detection receiver assuming signal reception over an additive white Gaussian noise (AWGN) channel. It is shown that receiver employing direct bit detection offers simpler hardware implementation and yet provide bit error rate comparable to that of the standard phase detection receiver.

Digital channel coding is a practical method of realizing high transmission reliability by introducing some form of error control on the transmitted information. In applications where the received signal-to-noise ratio is low such as encountered in satellite communication applications, error correction coding is usually a necessity for satisfactory system performance. Error correction is achieved by channel coding operation in which extra bits are systematically added to the output of the source encoder. While these extra bits by themselves convey no information, they make it possible for the receiver to detect and/or correct some of the errors present in the information bearing bits at the receiver.

There are two principal methods of performing the channel coding operation, namely block coding and convolutional coding. Both methods require storage and processing of binary data using a channel encoder and a channel decoder. While this requirement was a limiting factor in the early days of digital communications, it is no longer a critical problem because of the availability of solid state devices and memory at reasonable prices. The second part of the thesis is devoted to analyzing some examples of block and convolutional codes used in conjunction with the direct bit detection methods discussed in the first part of the thesis. These examples demonstrate that significant performance improvements (coding gains) in the order of 2 to 5 dB can be achieved with relatively simple block and convolutional codes.

II. PHASE DETECTION RECEIVER FOR M-ARY PSK

A. SIGNAL REPRESENTATION AND RECEIVER STRUCTURE

For M-ary phase-shift-keyed modulation with equal signal energies, a convenient representation of the signal set is given by

$$s_i(t) = \sqrt{2E_s/T}\cos(2\pi f_o t + 2\pi(i-1)/M), \qquad \text{(eqn 2.1)}$$
$$i = 1,2,\ldots,M; \quad 0 \le t \le T$$

where f_oT equals some integer. A suitable orthonormal signal set for the representation of M-ary PSK signals is given by

$$\varphi_1(t) = \sqrt{2/T}\cos 2\pi f_o t, \qquad \text{(eqn 2.2)}$$
$$\varphi_2(t) = \sqrt{2/T}\sin 2\pi f_o t, \quad 0 \le t \le T$$

Using trigonometric identity to expand $s_i(t)$ and expressing in terms of $\varphi_1(t)$ and $\varphi_2(t)$, we have

$$s_i(t) = \sqrt{E_s}\cos(2\pi(i-1)/M)\cdot\varphi_1(t) - \sqrt{E_s}\sin(\pi(i-1)/M)\cdot\varphi_2(t) \qquad \text{(eqn 2.3)}$$
$$i = 1,2,\ldots,M$$

A plot of the M-ary signal constellation can be made using $\varphi_1(t)$ and $\varphi_2(t)$ as axes for various values of M, where the coordinates of the ith signal vector is given by

$$[\sqrt{E_s}\cos(2\pi(i-1)/M), \sqrt{E_s}\sin(2\pi(i-1)/M)]$$

The signal constellation for 4-ary PSK (better known as QPSK) and 8-PSK are given in Figure 2.1 for illustration purposes.

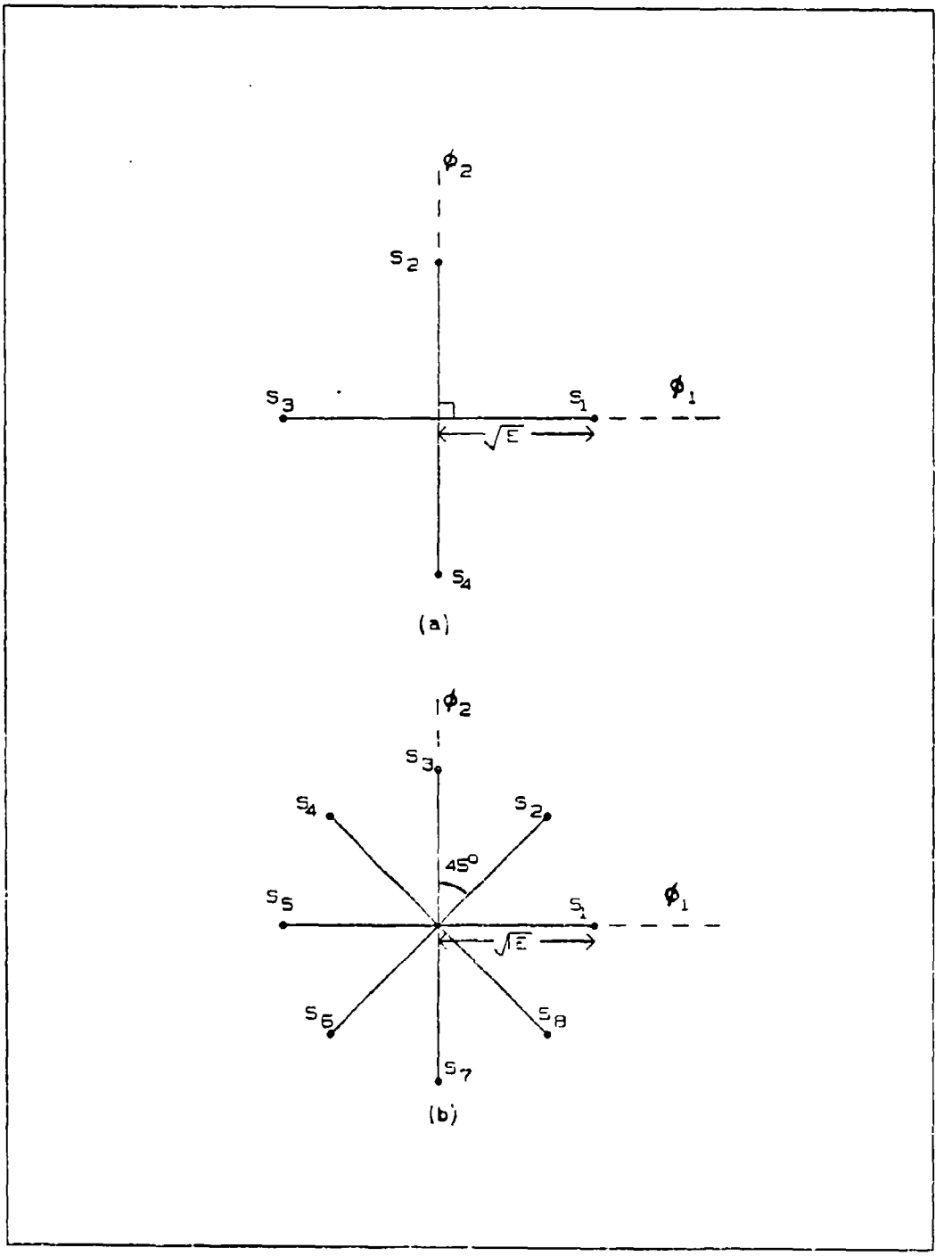

Figure 2.1 Signal constellations for (a) QPSK modulation (b) 8-PSK modulation

Since a general M-ary PSK signal can be expressed in terms of $\varphi_1(t)$ and $\varphi_2(t)$ and the decision criteria for the detection of the signal is based upon phase angle discrimination, a receiver using $\varphi_1(t)$ and $\varphi_2(t)$ as correlators followed by integration, sampling and phase computation is known to be optimum in minimum probability of error sense assuming each signal is equally likely to be transmitted, and the received signal is contaminated with additive white Gaussian noise (AWGN). The corresponding receiver structure is shown in Figure 2.2. The same receiver structure can also be obtained following a strict mathematical analysis as done in [Ref. 1: pp. 228-230].

Let the incoming signal over a T seconds interval be represented as

$$y(t) = s_k(t) + n(t), \quad 0 \le t \le T \qquad \text{(eqn 2.4)}$$

where

$$s_k(t) = \sqrt{2E_s/T}\cos(2\pi f_o t + 2\pi(k-1)/M), \qquad \text{(eqn 2.5)}$$
$$k = 1,2,\ldots,M$$

The output from the correlator-integrator is given by

$$Y_i = \int_0^T y(t)\varphi_i(t)dt, \quad i = 1,2 \qquad \text{(eqn 2.6)}$$

so that from eqn 2.4 and eqn 2.3, we have

$$Y_1 = \int_0^T [\sqrt{E_s/T}\cos(2\pi f_o t + 2\pi(k-1)/M) + n(t)]\varphi_1(t)\,dt \qquad \text{(eqn 2.7)}$$
$$= \sqrt{E_s}\cos(2\pi(k-1)/M) + N_c$$

where

$$N_c = \int_0^T n(t)\varphi_1(t)dt \qquad \text{(eqn 2.8)}$$

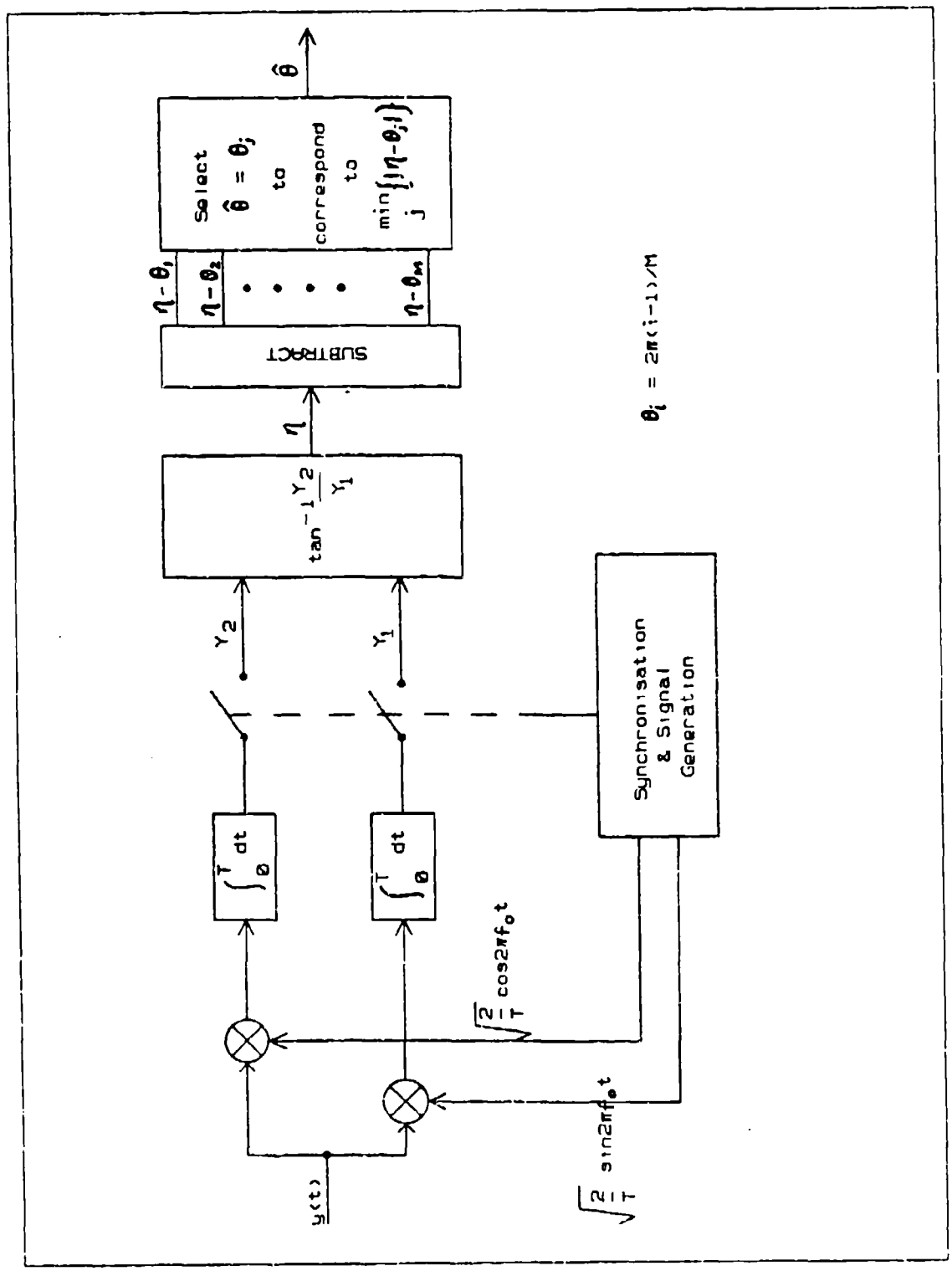

Figure 2.2 Receiver structure for M-ary PSK modulation

so that N_c is a Gaussian random variable with zero mean and variance $N_o/2$, which implies that Y_1 is Gaussian random variable with mean $\sqrt{E_s}\cos(2\pi(k-1)/M)$ and variance $N_o/2$, conditioned on $s_k(t)$ being transmitted. Similarly

$$Y_2 = \int_0^T [\sqrt{2E_s/T}\cos(2\pi f_o t + 2\pi(k-1)/M) + n(t)]\varphi_2(t)\,dt \qquad \text{(eqn 2.9)}$$

$$= -\sqrt{E_s}\sin(2\pi(k-1)/M) + N_s$$

where

$$N_s = \int_0^T n(t)\varphi_2(t)dt \qquad \text{(eqn 2.10)}$$

so that N_s has the same statistical properties as N_c implying that Y_2 is also a Gaussian random variable with mean $-\sqrt{E_s}\sin(2\pi(k-1)/M)$ and variance $N_o/2$, conditioned on $s_k(t)$ being transmitted. It can be shown that Y_1 and Y_2 are uncorrelated random variables, and since they are Gaussian, they are therefore statistically independent. Therefore their joint probability density function (pdf) is given by

$$p(y_1, y_2 | s_k(t)) = \qquad \text{(eqn 2.11)}$$

$$\frac{1}{\pi N_o} \exp\left[- \frac{(y_1 - \sqrt{E_s}\cos\theta_k)^2}{N_o} - \frac{(y_2 + \sqrt{E_s}\sin\theta_k)^2}{N_o} \right]$$

where $\theta_k = 2\pi(k-1)/M$. Transforming into polar coordinates using $Y_1 = R\cos\eta$ and $Y_2 = -R\sin\eta$, the pdf becomes

$$p(R,\eta | s_k(t)) = (R/\pi N_o)\exp(-(R^2 - 2R\sqrt{E_s}\cos(\eta-\theta_k) + E_s/N_o),$$

$$0 \le R \le \infty\ ,\ -\pi \le \eta \le \pi$$

$$= 0\ ,\ \text{otherwise} \qquad \text{(eqn 2.12)}$$

Integrating over R and writing $r = R/\sqrt{N_o}$, $d = E_s/N_o$, the pdf of the phase angle η becomes

$$p(\eta|s_k(t)) = (r/\pi)\exp(-(r^2 - 2r\sqrt{d}\cos(\eta-\theta_k) + d))\, dr, \quad -\pi \le \eta \le \pi \qquad \text{(eqn 2.13)}$$

$$= 0 \quad , \quad \text{elsewhere}$$

The probability of correctly detecting the kth signal denoted $Pr\{correct|s_k(t)\}$ is the probability that $|\theta_k-\eta|$ is the minimum for all $|\theta_j-\eta|$, $j = 1,2,\ldots,M$ or equivalently since $\theta_k = 2\pi(k-1)/M$, is the probability that η is in the region $[\ (2k-3)\pi/M\ ,\ (2k-1)\pi/M\ ]$, therefore

$$Pr\{correct|s_k(t)\} = \int_{\eta_1}^{\eta_2} p(\ \eta|s_k(t))\ d\eta \qquad \text{(eqn 2.14)}$$

where $\eta_1 = (2k-3)\pi/M$ and $\eta_2 = (2k-1)\pi/M$. If we substitute $\psi = \eta - 2\pi(k-1)/M$ in the above equation, we see that

$$Pr\{correct|s_k(t)\} = \int_{-\pi/M}^{\pi/M} p(\psi)\ d\psi \qquad \text{(eqn 2.15)}$$

which is independent of the index k. For equiprobable signals, the probability of correct decisions, denoted $P_c(M)$ becomes

$$P_c(M) = Pr\{correct|s_k(t)\} \text{ for any } k \qquad \text{(eqn 2.16)}$$

$$= (2/\pi)\exp(-d)\int_0^{\infty} r\ \exp(-r^2)\int_0^{\pi/M}\exp(2r\sqrt{d}\cos\psi)\ d\psi\ dr$$

$$= (2/\pi)\int_0^{\infty}\exp(-(u-\sqrt{d})^2)\int_0^{u\tan\pi/M}\exp(-v^2)\ dv\ du$$

where a change of variables using $u = r\cos\psi$, $v = r\sin\psi$ has been used in order to obtain the last equality. In the case of BPSK, namely M = 2, the probability of correct decision, $P_c(2)$, becomes

$$P_c(2) = (2/\pi)\int_0^{\infty}\exp(-(u-\sqrt{d}\ )^2)\int_0^{\infty}\exp(-v^2)\ dv\ du$$

$$= 1 - Q\ (\sqrt{2d}\ ) \qquad \text{(eqn 2.17)}$$

where Q(.)is the complimentary error function defined by

$$Q(x) = (1/\sqrt{2\pi}) \int_x^\infty \exp(-z^2/2)\, dz \qquad \text{(eqn 2.18)}$$

The symbol error probability denoted $P_E(2)$ which is the same as the bit error probability for M = 2, is given by

$$P_E(2) = 1 - P_c(2) = Q(\sqrt{2d}) \qquad \text{(eqn 2.19)}$$

$$= Q(\sqrt{2E_b/N_o})$$

since $E_b = E_s$ for BPSK.

B. RELATIONS BETWEEN SYMBOL AND BIT ERROR PROBABILITIES

As presented in the previous section, symbol error probabilities can be computed directly from knowledge of the channel characteristics and the derivation can be found in many references (see [Ref. 1: p. 231] for example). However, for transmission of binary data, and when comparing system with different levels of modulation, the bit error probability rather than the symbol error probability is of interest as explained in the introductory chapter. Unfortunately the computation of bit error probability is often quite complicated for multi-level modulation system and is often not carried or presented in most literature. In [Ref. 1: p. 198], the bit error probability has been determined only for the case of orthogonal signal sets where the result is

$$P_b(M) = 2^{n-1}.P_s(M)/(2^n - 1) \qquad \text{(eqn 2.20)}$$

with M = number of distinct signal waveforms

$P_s(M)$ = Symbol error probability of the transmitted signal

$P_b(M)$ = Bit error probability of the decoded data bit

n = $\log_2 M$

While Eqn. 2.20 shows the relationship between bit error probability and the symbol error probability, it is not applicable here because the M-ary PSK signal set is not orthogonal. Therefore, the remaining of this section is devoted to deriving the bit error probability for M-ary PSK signals. Using the notations previously introduced, and further defining p_k as the probability of k bits in error in a received n-bit data block where k = 1,2,...,n, then

$$P_s(M) = \sum_{k=1}^{n} p_k \qquad \text{(eqn 2.21)}$$

since the events {k errors in a block of n bits} are disjoint for k = 1,2,...,n. The average number of bits in error given that an n-bit symbol has been detected incorrectly is

$$\left(\sum_{k=1}^{n} kp_k \right) / \left(\sum_{k=1}^{n} p_k \right) \qquad \text{(eqn 2.22)}$$

Therefore the probability that a data bit is in error given that an n-bit symbol has been detected incorrectly denoted by P(B|S), is given by

$$P(B|S) = \left(\sum_{k=1}^{n} kp_k\right)/(nP_s(M)) \qquad \text{(eqn 2.23)}$$

Using Bayes' rule, we can write bit error probability $P_b(M)$ as

$$P_b(M) = P(B|S).P_s(M)/P(S|B) \qquad \text{(eqn 2.24)}$$

where P(S|B) is the probability of symbol error given that a bit error has occurred. Clearly this probability equal to 1, so that

$$P_b(M) = P(B|S).P_s(M) = \sum_{k=1}^{n} kp_k/n \qquad \text{(eqn 2.25)}$$

The main problem in the computation of bit error probability in the above equation is the determination of the p_k's which is a non-trivial task for multi-level modulation signals.

C. DERIVATION OF BIT ERROR PROBABILITIES FOR M-ARY PSK MODULATION

In general, the bit error probability depends on both the symbol error probability and the way in which a block of bits are grouped together to form the symbol waveforms prior to modulation of the carrier. One popular way of generating the symbols is the use of Gray code. Gray coding has the desirable property in that a given incorrect decision made on a symbol that is adjacent to the correct symbol is accompanied by one and only one bit error. This minimises the bit error rate since the main contribution to errors in symbol detection corresponds to incorrectly deciding in favor of the symbol adjacent to the actual transmitted symbol.

Examples of Gray coding for some M-ary modulation are shown in Figure 2.3 together with the bit error patterns based on the all zero symbol as reference. It is interesting to note that similar bit error patterns are obtained regardless of the codeword chosen as reference.

1. Bit error probability for QPSK

A simplified receiver structure for QPSK modulation is possible with the additional advantage of direct bit detection at no loss in performance [Ref. 2: pp. 120-124]. The receiver structure and the signal constellation with Gray coding assignments are shown in Figure 2.4.

From a close examination of the block diagram of the receiver structure for QPSK as shown in Figure 2.4(a), it is found that both the in-phase I channel producing the output Y_1 and decision a_1 and the quadrature Q channel producing the output Y_2 and decision a_2 are each similar to a BPSK demodulator. The I and Q channels provide direct detection of the 2-bit symbols associated with the QPSK modulation.

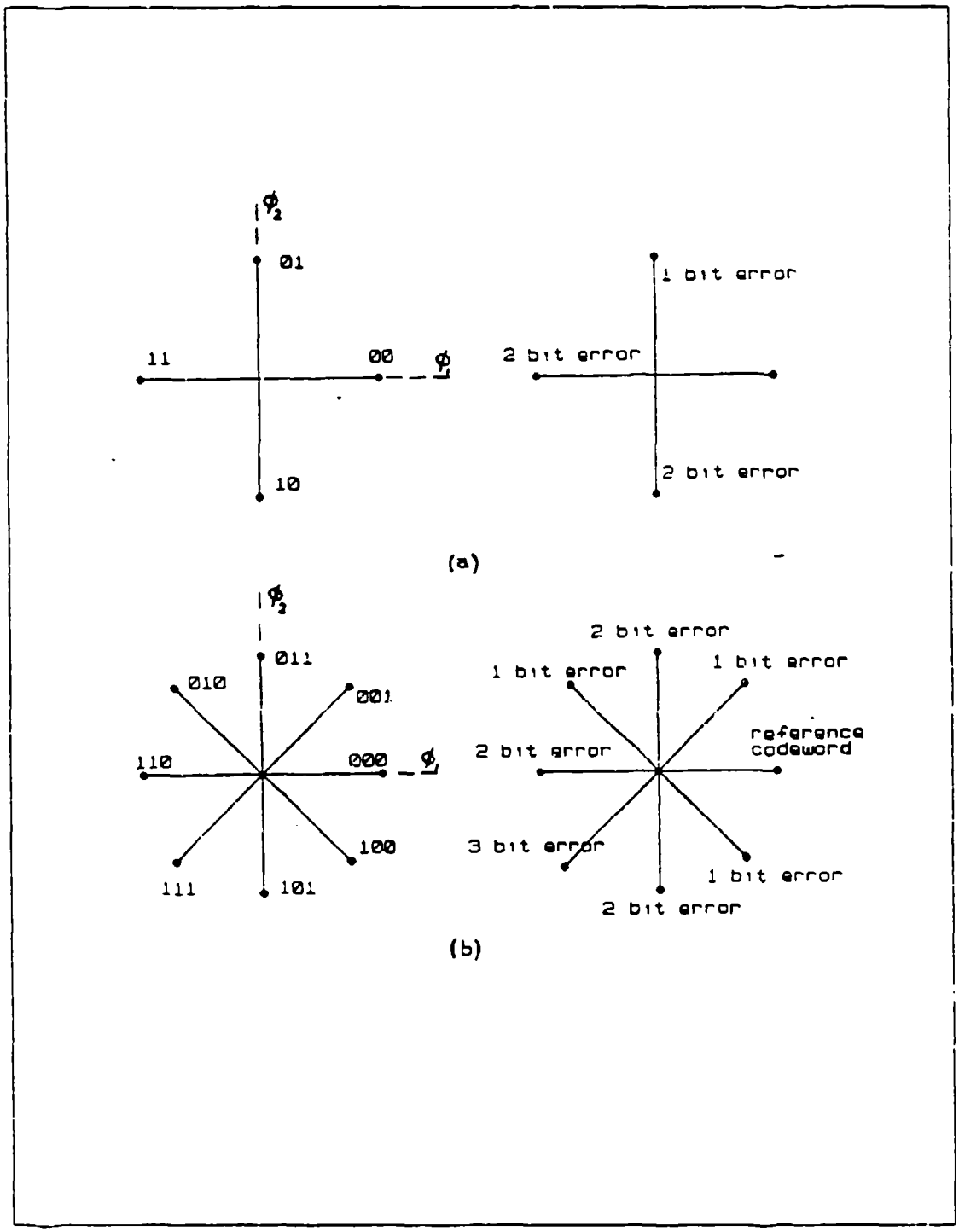

Figure 2.3 (a) Gray code assignment and bit error pattern for QPSK (b) Gray code assignment and bit error pattern for 8-PSK

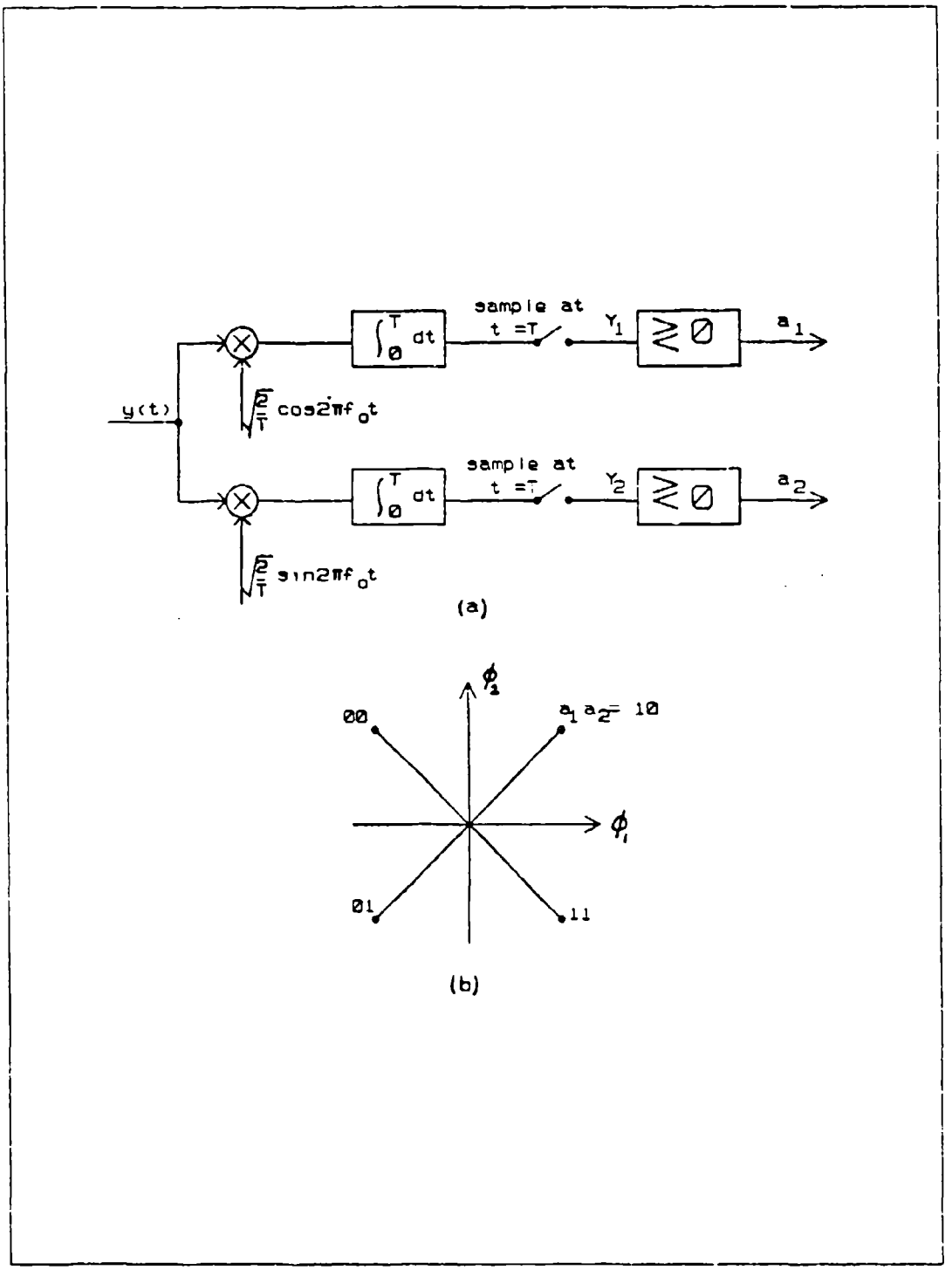

Figure 2.4 (a) Receiver structure for QPSK
(b) Gray code assignment and signal constellation for QPSK

Furthermore, the symbol error rate performance of the two orthogonal channels are the same. Therefore, the symbol error probability of each channel is given by

$$P_{eI} = P_{eQ} = P_{eBPSK} = Q(\sqrt{2E_b/N_o}) \qquad \text{(eqn 2.26)}$$

The bit error probability is obtained by observing that

$$\begin{aligned} p_1 &= \Pr\{ \text{ 1 bit error } \} \\ &= \Pr\{ a_1 \text{ and } a_2 \text{ but not both are in error } \} \\ &= 2Q(\sqrt{2E_b/N_o})[1 - Q(\sqrt{2E_b/N_o})] \end{aligned}$$

$$\begin{aligned} p_2 &= \Pr\{ \text{ 2 bit error } \} = \Pr\{ a_1 \text{ and } a_2 \text{ in error } \} \\ &= [Q(\sqrt{2E_b/N_o})]^2 \end{aligned}$$

so that the resulting bit error probability, $P_b(4)$ is given by

$$\begin{aligned} P_b(4) &= 0.5p_1 + p_2 \qquad \text{(eqn 2.27)} \\ &= Q(\sqrt{2E_b/N_o}) \end{aligned}$$

It is interesting to note that the bit error probability for a Gray coded QPSK is identical to that of BPSK where the same bit energy-to-noise ratio is maintained for both systems. This is a special case whereby there is no performance penalty in the bit error rate when a higher order of modulation is used in place of a lower modulation, namely QPSK in place of BPSK.

2. Bit error probability for 8-PSK signal

The bit error probability of the standard receiver structure shown in Figure 2.2 is now considered for the case of 8-PSK signal with arbitrary phase angle separation as shown in Figure 2.5. Define

$$\begin{aligned} p_1 &= \Pr\{ \text{ 1 bit error} | s_1(t) \} \\ &= \Pr\{s_2(t) | s_1(t)\} + \Pr\{s_4(t) | s_1(t)\} \\ &\quad + \Pr\{s_8(t) | s_1(t)\} \qquad \text{(eqn 2.28)} \end{aligned}$$

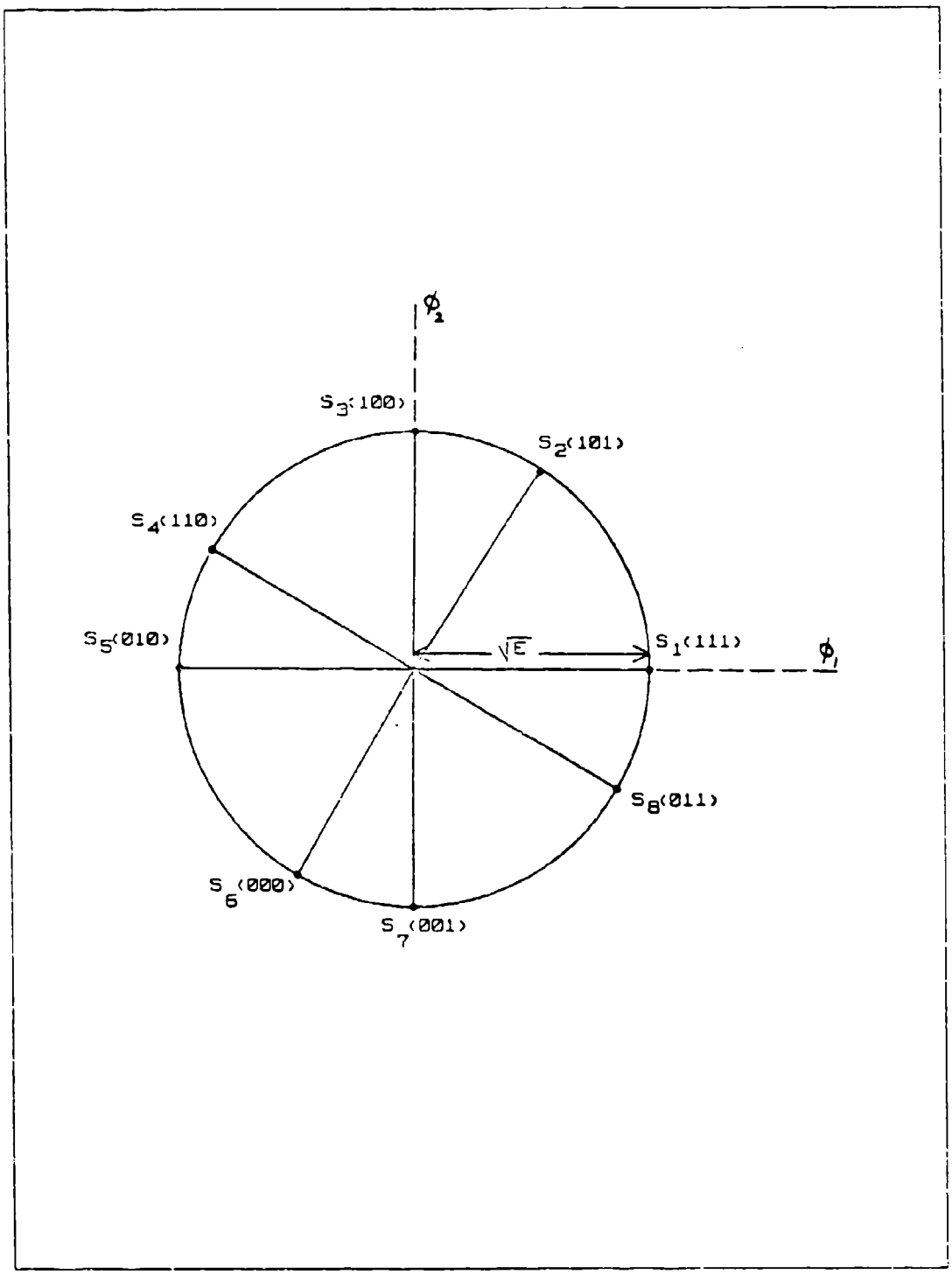

Figure 2.5 Signal constellation and Gray code assignments for arbitrary phase angle spacings 8-PSK signal

Considering each term individually in the Eqn. 2.28, we have

$$\Pr\{ s_2(t) | s_1(t) \} =$$

$$\Pr\left\{ n_1 \geq -\sqrt{E}\ ,\ (\sqrt{E} + n_1)\tan\tfrac{\beta}{2} \leq n_2 \leq (\sqrt{E} + n_1)\tan\left(\tfrac{\pi}{2} - \tfrac{\alpha}{2}\right) \right\}$$

$$= \int_{-\sqrt{E}}^{\infty} \frac{1}{\sqrt{\pi N_o}} e^{-n_1^2/N_o} \left[Q\left(\frac{(\sqrt{E} + n_1)\tan\beta/2}{\sqrt{N_o/2}} \right) - Q\left(\frac{(\sqrt{E} + n_1)\tan\left(\frac{\pi}{2} - \frac{\alpha}{2}\right)}{\sqrt{N_o/2}} \right) \right] dn_1$$

where n_1 and n_2 are the components of the additive white Gaussian noise along the $\varphi_1(t)$ and $\varphi_2(t)$ axis. Let $x^2/2 = N_1^2/N_o$, this implies

$$\Pr\{ s_2(t) | s_1(t) \} =$$

$$\int_{-\sqrt{2d}}^{\infty} \frac{1}{\sqrt{2\pi}} e^{-x^2/2} \left[Q\left((\sqrt{2d} + x)\tan\beta/2 \right) - Q\left((\sqrt{2d} + x)\tan\left(\tfrac{\pi}{2} - \tfrac{\alpha}{2}\right) \right) \right] dx$$

where $d = E/N_o$. Similarly, we can obtain

$$\Pr\{ s_4(t) | s_1(t) \} =$$

$$\int_{-\infty}^{-\sqrt{2d}} \frac{1}{\sqrt{2\pi}} e^{-x^2/2} \left[Q\left((\sqrt{2d} + x)\tan\tfrac{\alpha}{2} \right) - Q\left((\sqrt{2d} + x)\tan\left(\tfrac{\pi}{2} - \beta/2\right) \right) \right] dx$$

$$\Pr\{ s_8(t) | s_1(t) \} =$$

$$\int_{-\sqrt{2d}}^{\infty} \frac{1}{\sqrt{2\pi}} e^{-x^2/2} \left[Q\left((\sqrt{2d} + x)\tan\tfrac{\alpha}{2} \right) - Q\left((\sqrt{2d} + x)\tan\left(\tfrac{\pi}{2} - \beta/2\right) \right) \right] dx$$

Combining all the three terms of the above expression for the equation of p_1 given in Eqn. 2.28 and after some simplication, we obtain

$$p_1 = \Pr\{ 1 \text{ bit error} | s_1(t) \}$$

$$= \int_{-\sqrt{2d}}^{\infty} \frac{1}{\sqrt{2\pi}} e^{-x^2/2} \left[Q\left((\sqrt{2d} + x)\tan\beta/2 \right) - Q\left((\sqrt{2d} + x)\tan\left(\tfrac{\pi}{2} - \tfrac{\alpha}{2}\right) \right) \right] dx$$

$$+ \int_{-\infty}^{\infty} \frac{1}{\sqrt{2\pi}} e^{-x^2/2} \left[Q\left((\sqrt{2d} + x) \tan\frac{\alpha}{2} \right) - Q\left((\sqrt{2d} + x) \tan\left(\frac{\pi}{2} - \frac{\beta}{2}\right) \right] dx$$

Similarly.

$$P_2 = \Pr\{ \text{2 bit error} | s_1(t) \}$$

$$= \Pr\{s_3(t)|s_1(t)\} + \Pr\{s_5(t)|s_1(t)\} + \Pr\{s_7(t)|s_1(t)\}$$

$$= \int_{-\sqrt{2d}}^{\infty} \frac{1}{\sqrt{2\pi}} e^{-x^2/2} \left[Q\left((\sqrt{2d} + x) \tan\left(\frac{\pi}{2} - \frac{\alpha}{2}\right) \right] dx$$

$$+ \int_{-\infty}^{-\sqrt{2d}} \frac{1}{\sqrt{2\pi}} e^{-x^2/2} \left[Q\left((\sqrt{2d} + x) \tan\left(\frac{\pi}{2} - \frac{\beta}{2}\right) \right) \right] dx$$

$$+ \int_{-\infty}^{-\sqrt{2d}} \frac{1}{\sqrt{2\pi}} e^{-x^2/2} \left[Q\left(-(\sqrt{2d} + x) \tan\frac{\beta}{2} \right) - Q\left((\sqrt{2d} + x) \tan\frac{\alpha}{2} \right) \right] dx$$

$$+ \int_{-\infty}^{-\sqrt{2d}} \frac{1}{\sqrt{2\pi}} e^{-x^2/2} \left[Q\left((\sqrt{2d} + x) \tan\left(\frac{\pi}{2} - \frac{\alpha}{2}\right) \right) \right] dx$$

$$+ \int_{-\sqrt{2d}}^{\infty} \frac{1}{\sqrt{2\pi}} e^{-x^2/2} \left[Q\left((\sqrt{2d} + x) \tan\left(\frac{\pi}{2} - \frac{\beta}{2}\right) \right) \right] dx$$

$$= \int_{-\infty}^{\infty} \frac{1}{\sqrt{2\pi}} e^{-x^2/2} \left[Q\left((\sqrt{2d} + x) \tan\left(\frac{\pi}{2} - \frac{\alpha}{2}\right) \right) - Q\left((\sqrt{2d} + x) \tan\left(\frac{\pi}{2} - \frac{\beta}{2}\right) \right) \right] dx$$

$$+ \int_{-\infty}^{-\sqrt{2d}} \frac{1}{\sqrt{2\pi}} e^{-x^2/2} \left[Q\left(-(\sqrt{2d} + x) \tan\frac{\beta}{2} \right) - Q\left((\sqrt{2d} + x) \tan\frac{\alpha}{2} \right) \right] dx$$

Finally,

$$P_3 = \Pr\{ \text{3 bit error} | s_1(t) \}$$

$$= \Pr\{ s_5(t) | s_1(t) \}$$

$$= \int_{-\infty}^{-\sqrt{2d}} \frac{1}{\sqrt{2\pi}} e^{-x^2/2} \left[Q\left((\sqrt{2d} + x) \tan\frac{\beta}{2} \right) - Q\left((\sqrt{2d} + x) \tan\left(\frac{\pi}{2} - \frac{\alpha}{2}\right) \right) \right] dx$$

Furthermore, it can be shown that the same expressions for p_1, p_2, p_3, are obtained when conditioned on the other signal $s_i(t)$ being transmitted, i = 2,3,...,8 so that the bit error probability $P_b(8)$ becomes

$$P_b(8) = p_1/3 + 2p_2/3 + p_3 \qquad \text{(eqn 2.29)}$$

Bit error probabilities with different values of α and β were computed with the aid of a computer. It can be verified from the numerical results that the lowest bit error rate occurs for the case of equal angle spacing, i.e., $\alpha = 45^\circ$. The bit error probabilities for the cases $\alpha = 30^\circ, 36^\circ, 45^\circ, 54^\circ, 60^\circ$ have been plotted as shown in Figure 2.6.

3. Bit error probability for 16-PSK signal

The performance of the receiver shown in Figure 2.2 was analyzed for 16-PSK modulation having the signal constellation shown in Figure 2.7. Observe the use of equal angle separation for the signal vectors with Gray bit codes assigned to the signals.

Assuming that the transmitted signal is $s_1(t)$, then

$$p_1 = \Pr\{\text{one bit error} | s_1(t)\}$$

$$= \Pr\{s_2(t)|s_1(t)\} + \Pr\{s_4(t)|s_1(t)\}$$

$$+ \Pr\{s_8(t)|s_1(t)\} + \Pr\{s_{16}(t)|s_1(t)\}$$

$$= 2\int_{-\sqrt{2d}}^{\infty} \frac{1}{\sqrt{2\pi}} e^{-x^2/2} \left[Q\left((\sqrt{2d}+x)\tan 11.25^\circ\right) - Q\left((\sqrt{2d}+x)\tan 33.75^\circ\right)\right] dx$$

$$+ \int_{-\sqrt{2d}}^{\infty} \frac{1}{\sqrt{2\pi}} e^{-x^2/2} \left[Q\left((\sqrt{2d}+x)\tan 56.25^\circ\right) - Q\left((\sqrt{2d}+x)\tan 78.75^\circ\right)\right] dx$$

$$+ \int_{-\infty}^{-\sqrt{2d}} \frac{1}{\sqrt{2\pi}} e^{-x^2/2} \left[Q\left((\sqrt{2d}+x)\tan 11.25^\circ\right) - Q\left((\sqrt{2d}+x)\tan 33.75^\circ\right)\right] dx$$

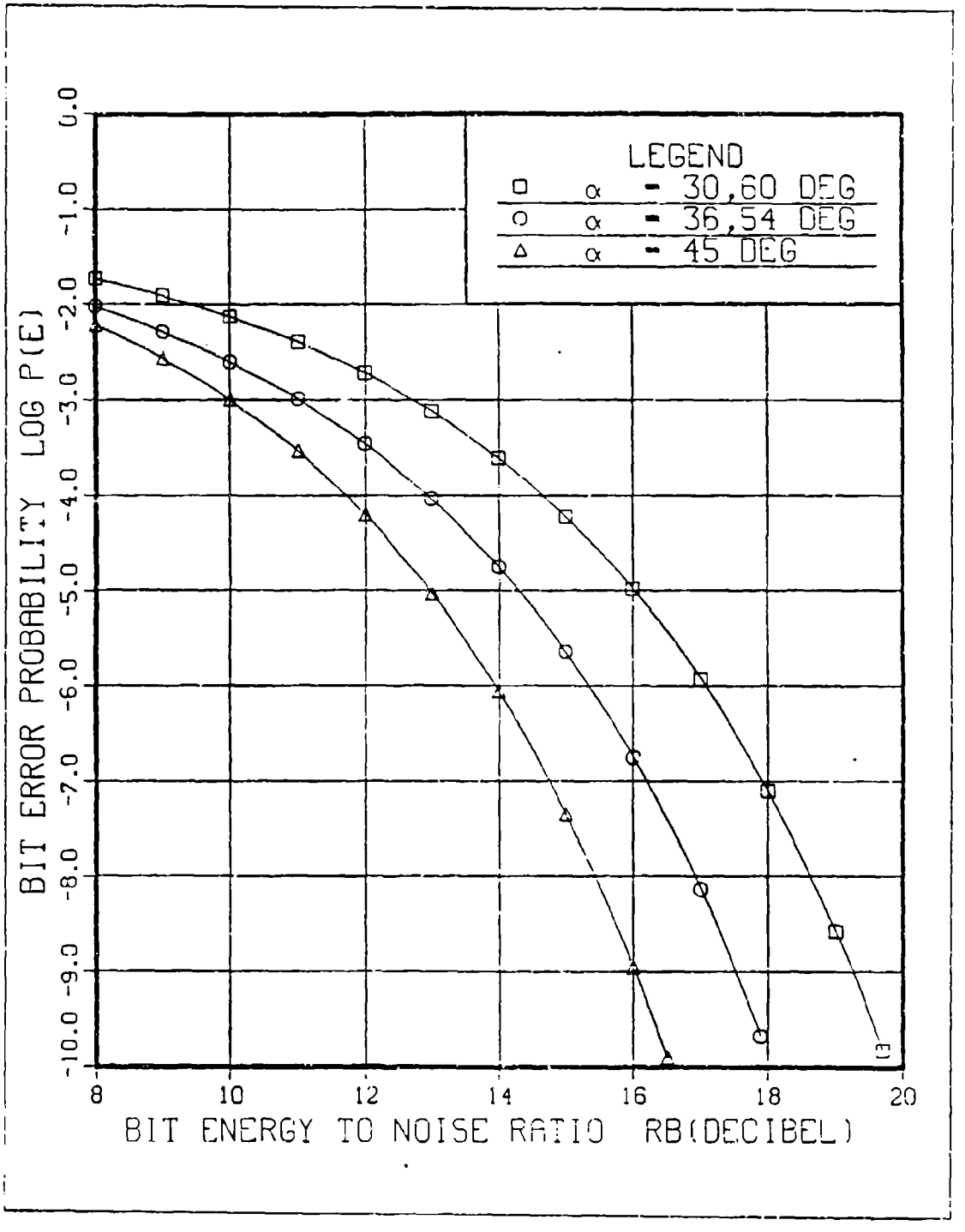

Figure 2.6 Bit error probabilities for 8-PSK standard phase detector with different phase angle spacing

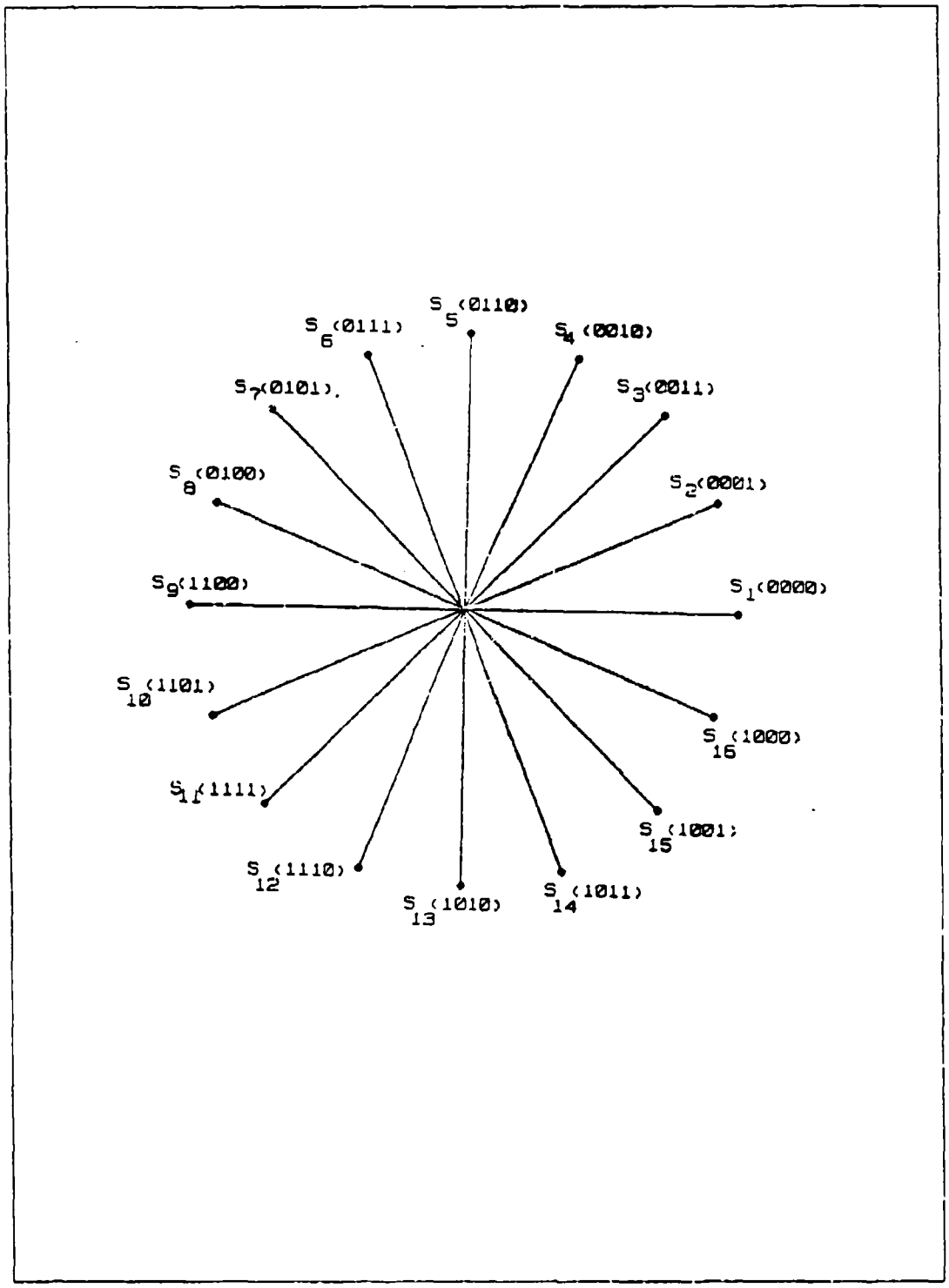

Figure 2.7 Signal constellation for 16-PSK signal

Similarly

$$p_2 = \Pr\{\text{2 bit error} \mid s_1(t)\}$$

$$= \Pr\{s_3(t)|s_1(t)\} + \Pr\{s_5(t)|s_1(t)\} + \Pr\{s_7(t)|s_1(t)\}$$

$$+ \Pr\{s_9(t)|s_1(t)\} + \Pr\{s_{13}(t)|s_1(t)\} + \Pr\{s_{15}(t)|s_1(t)\}$$

$$= 2\int_{-\sqrt{2d}}^{\infty} \frac{1}{\sqrt{2\pi}} e^{-x^2/2} \left[Q\left((\sqrt{2d}+x)\tan 33.75^\circ\right) - Q\left((\sqrt{2d}+x)\tan 56.25^\circ\right)\right] dx$$

$$+ 2\int_{-\infty}^{\infty} \frac{1}{\sqrt{2\pi}} e^{-x^2/2} \left[Q\left((\sqrt{2d}+x)\tan 78.75^\circ\right)\right] dx$$

$$+ \int_{-\infty}^{-\sqrt{2d}} \frac{1}{\sqrt{2\pi}} e^{-x^2/2} \left[Q\left((\sqrt{2d}+x)\tan 33.75^\circ\right) - Q\left((\sqrt{2d}+x)\tan 56.25^\circ\right)\right] dx$$

$$+ \int_{-\infty}^{-\sqrt{2d}} \frac{1}{\sqrt{2\pi}} e^{-x^2/2} \left[Q\left((\sqrt{2d}+x)\tan(-11.25^\circ)\right) - Q\left((\sqrt{2d}+x)\tan 11.25^\circ\right)\right] dx$$

Also

$$p_3 = \Pr\{\text{3 bit error} \mid s_1(t)\}$$

$$= \Pr\{s_6(t)|s_1(t)\} + \Pr\{s_{10}(t)|s_1(t)\}$$

$$= \Pr\{s_{12}(t)|s_1(t)\} + \Pr\{s_{14}(t)|s_1(t)\}$$

$$= 2\int_{-\infty}^{-\sqrt{2d}} \frac{1}{\sqrt{2\pi}} e^{-x^2/2} \left[Q\left((\sqrt{2d}+x)\tan 56.25^\circ\right) - Q\left((\sqrt{2d}+x)\tan 78.75^\circ\right)\right] dx$$

$$+ \int_{-\infty}^{-\sqrt{2d}} \frac{1}{\sqrt{2\pi}} e^{-x^2/2} \left[Q\left((\sqrt{2d}+x)\tan 11.25^\circ\right) - Q\left((\sqrt{2d}+x)\tan 33.75^\circ\right)\right] dx$$

$$+ \int_{-\sqrt{2d}}^{\infty} \frac{1}{\sqrt{2\pi}} e^{-x^2/2} \left[Q\left((\sqrt{2d}+x)\tan 56.25^\circ\right) - Q\left((\sqrt{2d}+x)\tan 78.75^\circ\right)\right] dx$$

and finally

$$p_4 = \Pr\{ \text{4 bit error} | s_1(t) \}$$

$$= \Pr\{ s_{11}(t) | s_1(t) \}$$

$$= \int_{-\infty}^{-\sqrt{2d}} \frac{1}{\sqrt{2\pi}} e^{-x^2/2} \left[Q\left((\sqrt{2d} + x) \tan 33.75^\circ \right) - Q\left((\sqrt{2d} + x) \tan 56.25^\circ \right) \right] dx$$

It can be shown that the same expressions for p_1, p_2, p_3, and p_4 are obtained conditioned on all other signal $s_i(t)$ being transmitted, $i = 2,\ldots,16$. Thus, the bit error probability becomes

$$P_b(16) = p_1/4 + p_2/2 + 3p_3/4 + p_4 \qquad \text{(eqn 2.30)}$$

When the above integral expression for p_1, p_2, p_3, and p_4 were evaluated numerically on a computer, it was found that for $d = E/N_o \geq 5$ dB, the integrals whose limits range from negative infinity to $-\sqrt{2d}$ were so small that no difference in the overall results were obtained by ignoring their contribution even when using double precision computation on the IBM 3033 computer. The bit error probabilities of 16-PSK were plotted in Figure 2.8 along with those obtained from equal angle spacing 8-PSK and QPSK. The curves were plotted using bit energy-to-noise ratio on the horizontal axis thereby providing a fair basis for comparing the different levels of signal modulation. It can be observed from the curves that bit error rate performance deteriorates with higher order M-ary modulation which is an expected result. At bit error rate of 10^{-5} or less, the performance loss is about 3.5 dB between QPSK and 8-PSK and 4.5 dB between 8-PSK and 16-PSK.

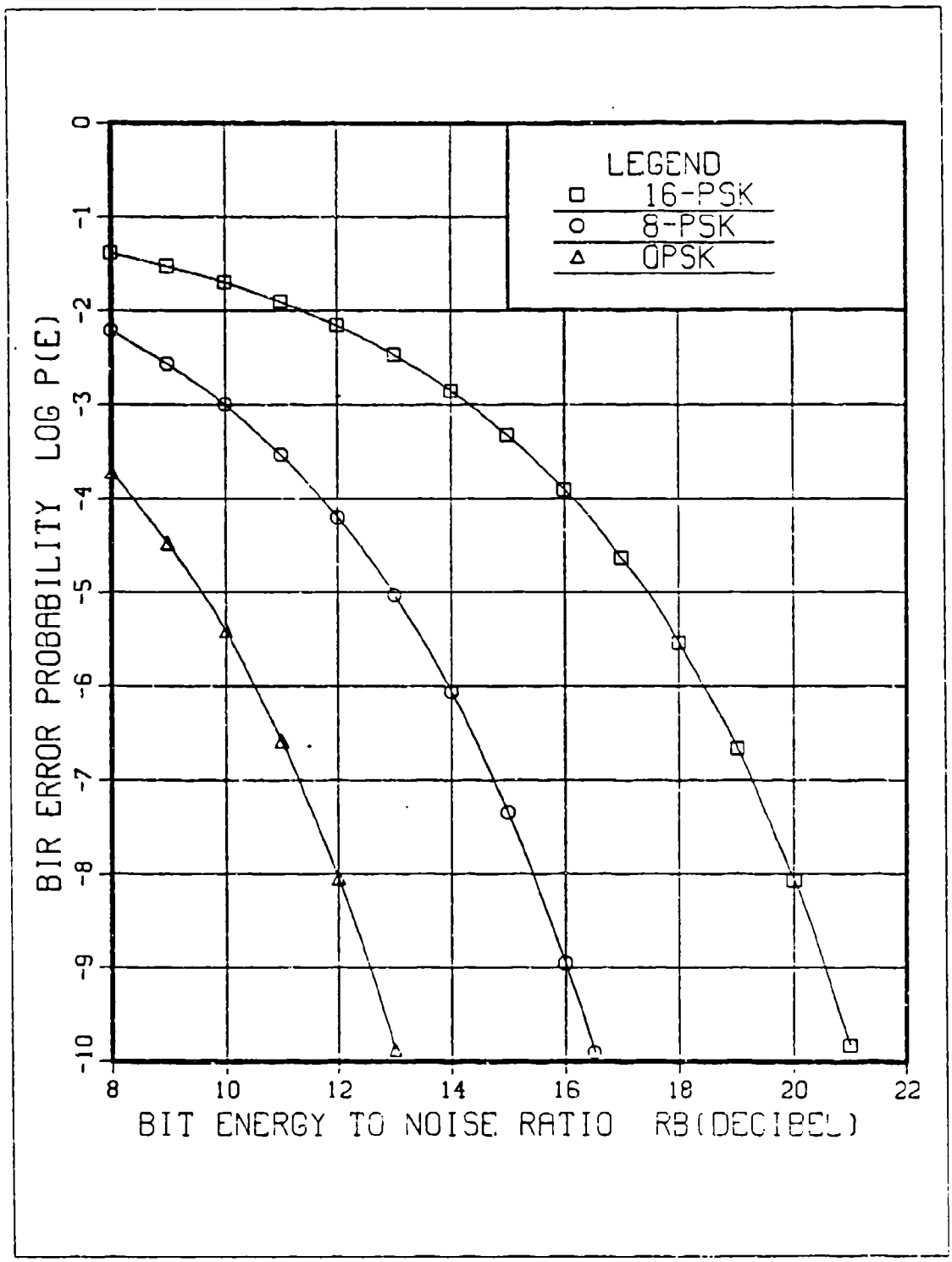

Figure 2.8 Bit error probabilities vs E_b/N_o for 16-PSK, 8-PSK and QPSK

III. BIT DETECTION RECEIVERS FOR M-ARY PSK

In Chapter 2, it has been demonstrated that direct bit detection can be achieved with QPSK signalling at no loss in bit error rate performance. This approach of direct bit detection will be extended to 8-PSK and 16-PSK modulation by suggesting possible receiver structures and computing their bit error probabilities. The results are then compared with those obtained from the standard phase detection receivers.

A. DIRECT BIT DETECTION FOR 8-PSK

The signal constellation for 8-PSK modulation with Gray bit coding assignment and the receiver structure for direct bit detection were shown in Figure 3.1. For the Gray bit coding assignment, it can be seen that the detection of the most significant bit (MSB) requires a decision as to whether the received signal vector falls on the upper or lower half of the signal space. The detection of the least significant bit (LSB) requires a similar decisions as to whether the signal vector is in the left half or right half of the signal space. The detection of the middle bit is slightly more complicated. The received signal component along the $\varphi_1(t)$ axis is squared and compared to a threshold in order to determine whether it is a logical 0's or a logical 1's. From the signal space diagram, we see that for the two signal vectors that lie in the same quadrant, the components along the φ_1 axis are given by $\pm\sqrt{E}\cos\alpha/2$ or $\pm\sqrt{E}\sin\alpha/2$. It would therefore be appropriate to choose the threshold at

$$0.5[E\cos^2(\alpha/2) + E\sin^2(\alpha/2)] = E/2$$

Such a receiver structure provides a simplification in hardware implementation over that of a standard phase detector and was first proposed by Thompson [Ref. 3].

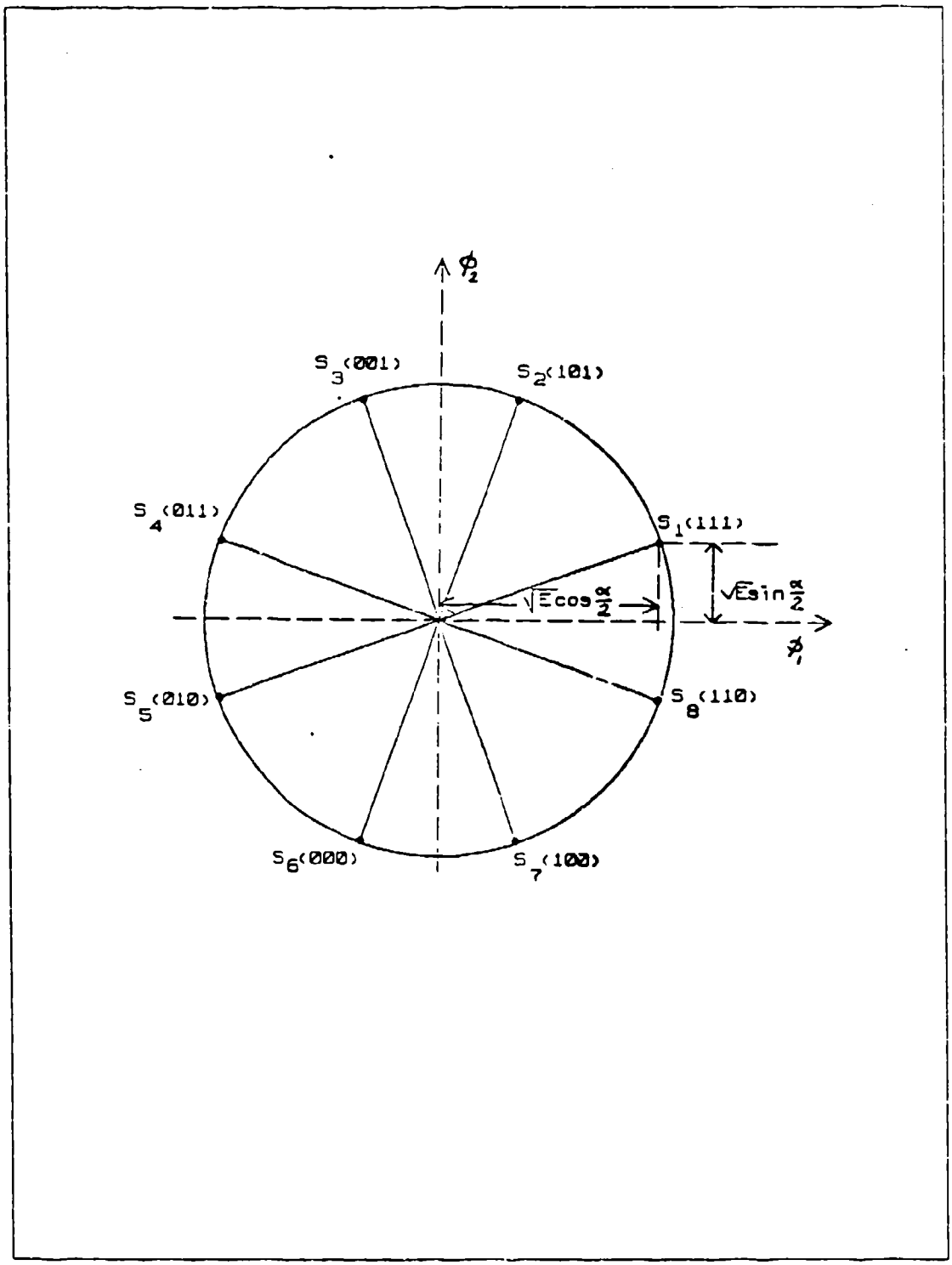

Figure 3.1 (a) Signal constellation for 8-PSK with arbitrary phase angle spacing

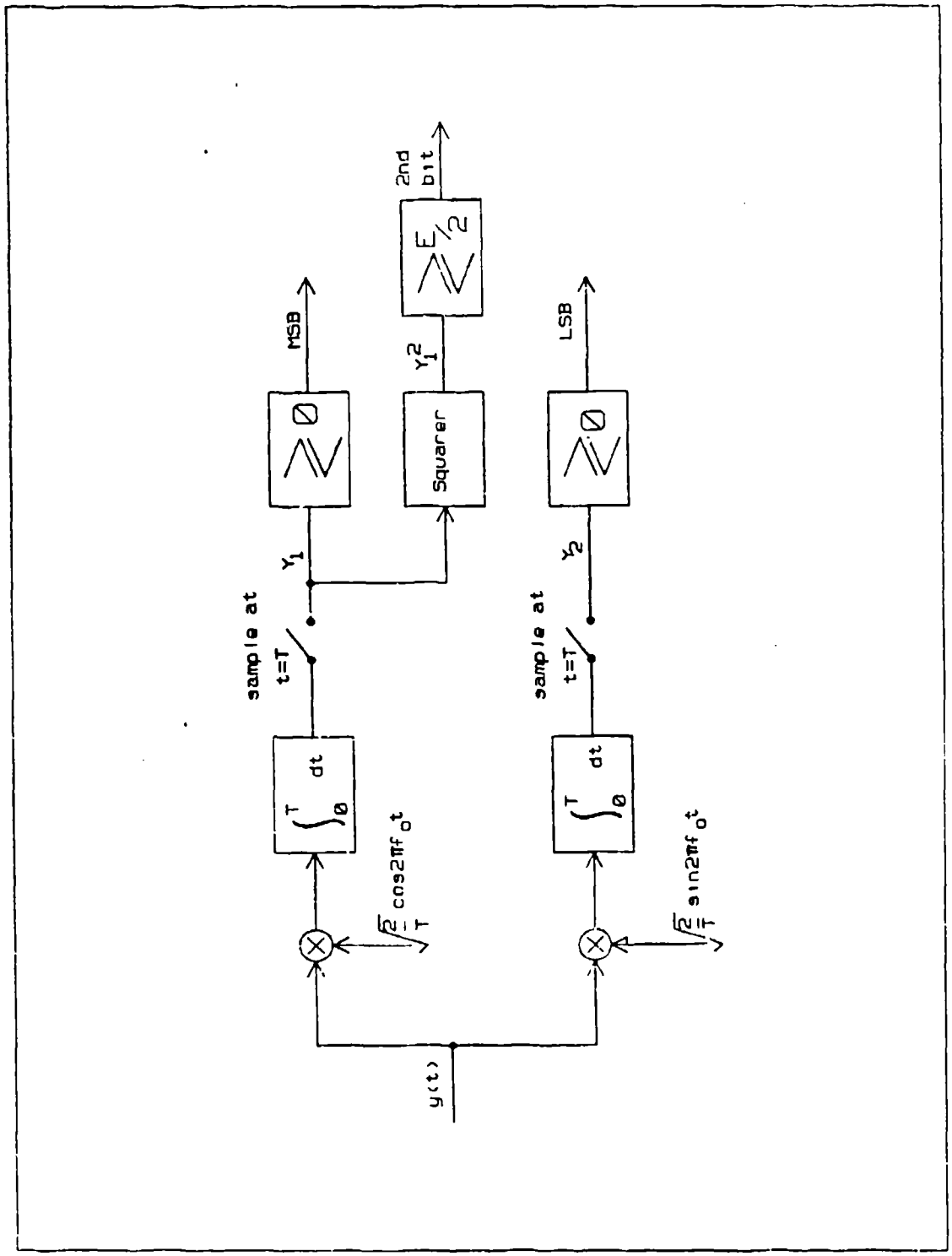

Figure 3.1 (b) Receiver structure for direct bit detection of 8-PSK

Thompson constructed the receiver structure of Figure 3.1(b) and carried out an experimental evaluation of the system's bit error rate performance at two angle settings, namely $\alpha = 36.8^{\circ}$ and $\alpha = 45^{\circ}$ (equal angle spacing). The experimental results demonstrated that the phase angle setting at $\alpha = 36.8^{\circ}$ gave a better bit error rate performance than for equal angle spacing. The experimental results were however not supported by any analytical studies.

In the following, analytical results are presented in order to evaluate the bit error rate at arbitrary phase angle spacings between signals for the receiver proposed by Thompson. The optimum phase angle spacing was computed and the bit error rate compared to that of a standard phase detection receiver.

Define p_{em} = Pr{ MSB error } and n_1 as the noise component along the $\varphi_1(t)$ axis. Using the symmetrical properties of signal vectors about the $\varphi_1(t)$ and $\varphi_2(t)$ axes, we need only consider the two cases conditioned on $s_1(t)$ and $s_2(t)$ being transmitted. This together with the condition of equiprobable signals allowed p_{em} to be written as

$$p_{em} = 0.5[\ \Pr\{\text{MSB error}|s_1(t)\} + \Pr\{\text{MSB error}|s_2(t)\}\ ]$$

$$= \frac{1}{2}\int_{-\infty}^{-\sqrt{E}\sin\alpha/2} \frac{1}{\sqrt{\pi N_0}} e^{-n_1^2/N_0}\, dn_1 + \frac{1}{2}\int_{-\infty}^{-\sqrt{E}\cos\alpha/2} \frac{1}{\sqrt{\pi N_0}} e^{-n_1^2/N_0}\, dn_1$$

$$= \frac{1}{2} Q\left(\sqrt{\frac{2E}{N_0}}\sin\frac{\alpha}{2}\right) + \frac{1}{2} Q\left(\sqrt{\frac{2E}{N_0}}\cos\frac{\alpha}{2}\right) \qquad \text{(eqn 3.1)}$$

Similarly, it can be shown that with p_{el} = Pr{LSB error}, $p_{el} = p_{em}$. For the detection of the middle bit, we proceed with the following analysis

$$p(y_1 | s_i(t)) = \frac{1}{\sqrt{\pi N_0}} \exp\left(-\frac{(y_1 - s_{i1})^2}{N_0}\right); \quad i = 1, 2.$$

where s_{i1} is the component of signal $s_i(t)$ along the φ_1 axis. Define $z = y_1^2$, so that

$$p(z|s_i(t)) = \frac{1}{2\sqrt{\pi N_0 z}} \left[\exp\left(-\frac{(z - 2s_{i1}\sqrt{z} + s_{i1}^2)}{N_0}\right) + \exp\left(-\frac{(z + 2s_{i1}\sqrt{z} + s_{i1}^2)}{N_0}\right)\right]; \; z \geq 0$$

$$= 0 \; ; \; otherwise$$

Define p_{ei} = Pr{middle bit error}. It can be shown that like the case of p_{em}, we need only consider the two cases conditioned on $s_1(t)$ and $s_2(t)$ being transmitted so that

$$p_{ei} = 0.5\{ \Pr\{\text{middle bit error} | s_1(t)\} + \Pr\{\text{middle bit error} | s_2(t)\} \}$$

$$= 0.5\left[\int_0^{E/2} p(z|s_1(t))dz + \int_{E/2}^{\infty} p(z|s_2(t))dz \right] \qquad \text{(eqn 3.2)}$$

Analyzing each term separately, we have

$$\int_0^{E/2} p(z|s_i(t))\,dz = \int_0^{E/2} \frac{1}{2\sqrt{\pi N_0 z}} \exp\left(-\frac{(z - 2s_{i1}\sqrt{z} + s_{i1}^2)}{N_0}\right) dz + \int_0^{E/2} \frac{1}{2\sqrt{\pi N_0 z}} \exp\left(-\frac{(z + 2s_{i1}\sqrt{z} + s_{i1}^2)}{N_0}\right) dz$$

$$= \int_0^{\sqrt{E/2}} \frac{1}{\sqrt{\pi N_0}} \exp\left(-\frac{(x^2 - 2s_{i1}x + s_{i1}^2)}{N_0}\right) dx + \int_0^{\sqrt{E/2}} \frac{1}{\sqrt{\pi N_0}} \exp\left(-\frac{(x^2 + 2s_{i1}x + s_{i1}^2)}{N_0}\right) dx$$

where the substitution $x = \sqrt{z}$ has been made. Normalising the integrand to a normal Gaussian distribution with zero mean and unit variance, we obtain

$$\int_0^{E/2} p\left(z \mid S_1(t)\right) dz = \int_{-S_{11}/\sqrt{N_0/2}}^{\sqrt{E/N_0} - S_{11}/\sqrt{N_0/2}} \frac{1}{\sqrt{2\pi}} e^{-x^2/2}\, dx + \int_{S_{11}/\sqrt{N_0/2}}^{\sqrt{E/N_0} + S_{11}/\sqrt{N_0/2}} \frac{1}{\sqrt{2\pi}} e^{-x^2/2}\, dx$$

$$= Q\left(-\frac{S_{11}}{\sqrt{N_0/2}}\right) - Q\left(\sqrt{\frac{E}{N_0}} - \frac{S_{11}}{\sqrt{N_0/2}}\right) + Q\left(\frac{S_{11}}{\sqrt{N_0/2}}\right) - Q\left(\sqrt{\frac{E}{N_0}} + \frac{S_{11}}{\sqrt{N_0/2}}\right)$$

$$= 1 - Q\left(\sqrt{\frac{E}{N_0}} - \sqrt{\frac{2E}{N_0}} \cos\frac{\alpha}{2}\right) - Q\left(\sqrt{\frac{E}{N_0}} + \sqrt{\frac{2E}{N_0}} \cos\frac{\alpha}{2}\right)$$

Furthermore

$$\int_{E/2}^{\infty} p\left(z \mid S_2(t)\right) dz = \int_{\sqrt{E/2}}^{\infty} \frac{1}{\sqrt{\pi N_0}} \exp\left(-\frac{(x^2 - 2S_{21}x + S_{21}^2)}{N_0}\right) dx + \int_{\sqrt{E/2}}^{\infty} \frac{1}{\sqrt{\pi N_0}} \exp\left(-\frac{(x^2 + 2S_{21}x + S_{21}^2)}{N_0}\right) dx$$

$$= Q\left(\sqrt{\frac{E}{N_0}} - \frac{S_{21}}{\sqrt{N_0/2}}\right) + Q\left(\sqrt{\frac{E}{N_0}} + \frac{S_{21}}{\sqrt{N_0/2}}\right)$$

$$= Q\left(\sqrt{\frac{E}{N_0}} - \sqrt{\frac{2E}{N_0}} \sin\frac{\alpha}{2}\right) + Q\left(\sqrt{\frac{E}{N_0}} + \sqrt{\frac{2E}{N_0}} \sin\frac{\alpha}{2}\right)$$

so that

$$P_{ei} = \frac{1}{2}\left[1 - Q\left(\sqrt{\frac{E}{N_0}} - \sqrt{\frac{2E}{N_0}} \cos\frac{\alpha}{2}\right) - Q\left(\sqrt{\frac{E}{N_0}} + \sqrt{\frac{2E}{N_0}} \cos\frac{\alpha}{2}\right)\right] + \frac{1}{2}\left[Q\left(\sqrt{\frac{E}{N_0}} - \sqrt{\frac{2E}{N_0}} \sin\frac{\alpha}{2}\right) + Q\left(\sqrt{\frac{E}{N_0}} + \sqrt{\frac{2E}{N_0}} \sin\frac{\alpha}{2}\right)\right]$$

We obtain finally the bit error probability $P_b(8)$ from

$$P_b(8) = 2P_{em}/3 + P_{ei}/3 \qquad \text{(eqn 3.3)}$$

The bit error probability ($P_b(E)$) versus bit energy-to-noise ratio (E_b/N_o) has been plotted over the range of α between 28^o and 40^o running in 2^o step increments and the results shown in Figure 3.2. An interesting result to note is that the bit error rate is not optimum at equal phase angle spacing. Using a computer search algorithm, it was found that the phase angle spacing for optimum performance varies over a small range of values depending on the size of the bit energy-to-noise ratio. The optimum phase angle versus the desired bit error rate (and its corresponding E_b/N_o) were tabulated in Table 1. It can be seen from the values tabulated that for lower E_b/N_o (i.e., values smaller than 13.2 dB), the optimum phase angle α equals 36^o. At higher E_b/N_o, the optimum phase angle α decreases and equal 32^o for $P_b(E) \leq 10^{-5}$, which represents a nominal design figure for most applications.

TABLE 1

OPTIMUM ANGLE SPACING VERSUS DESIRED BIT ERROR RATE

$P_b(E)$	E_b/N_o (dB)	Optimum α
5.10^{-3} - 6.10^{-4}	10.7 - 13.2	36^o
6.10^{-4} - 2.10^{-5}	13.2 - 15.7	34^o
$< 2.10^{-5}$	> 15.7	32^o

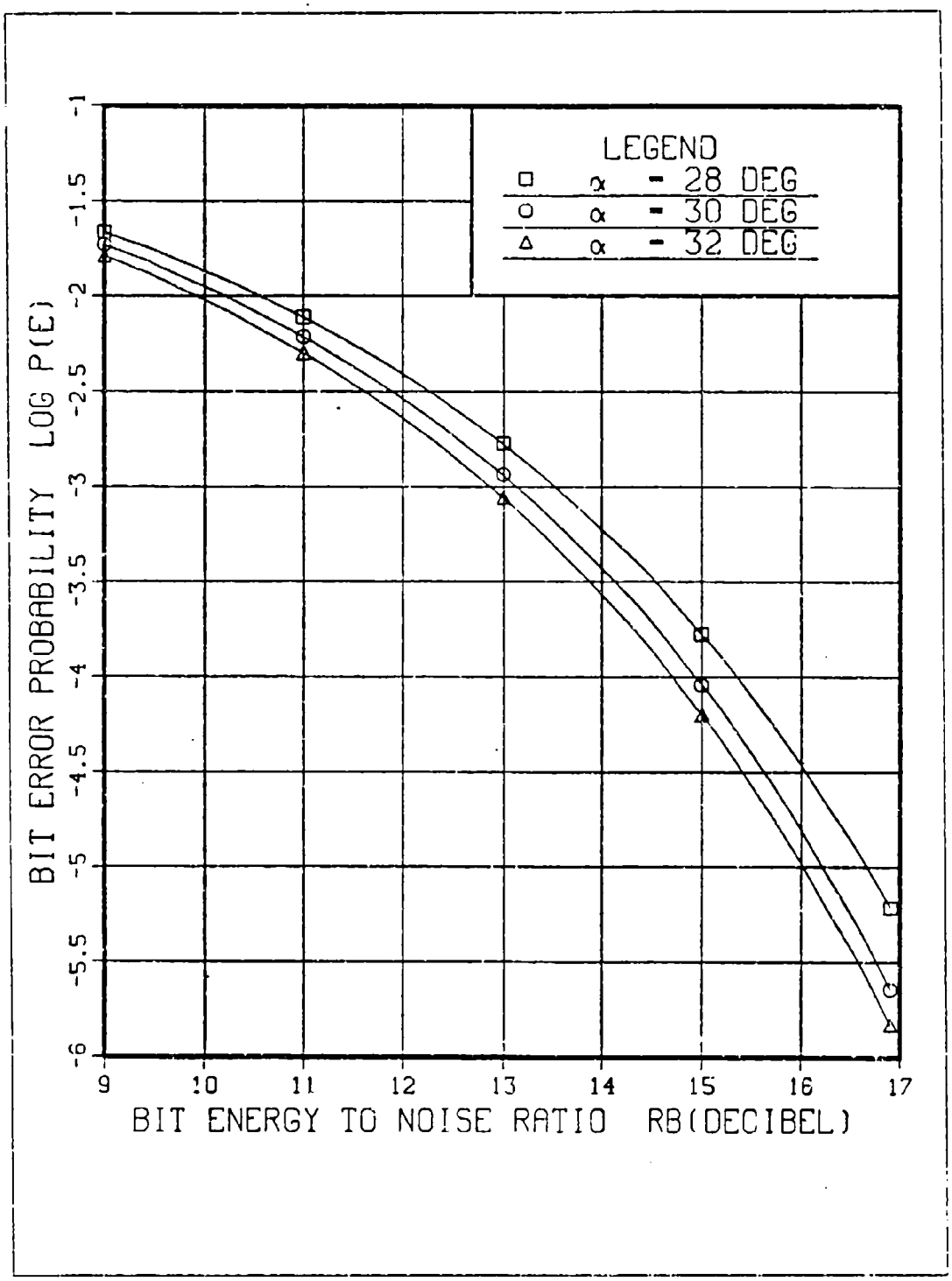

Figure 3.2 (a) Bit error probabilities for 8-PSK with bit detection receiver $\alpha = 28^{\circ} - 32^{\circ}$

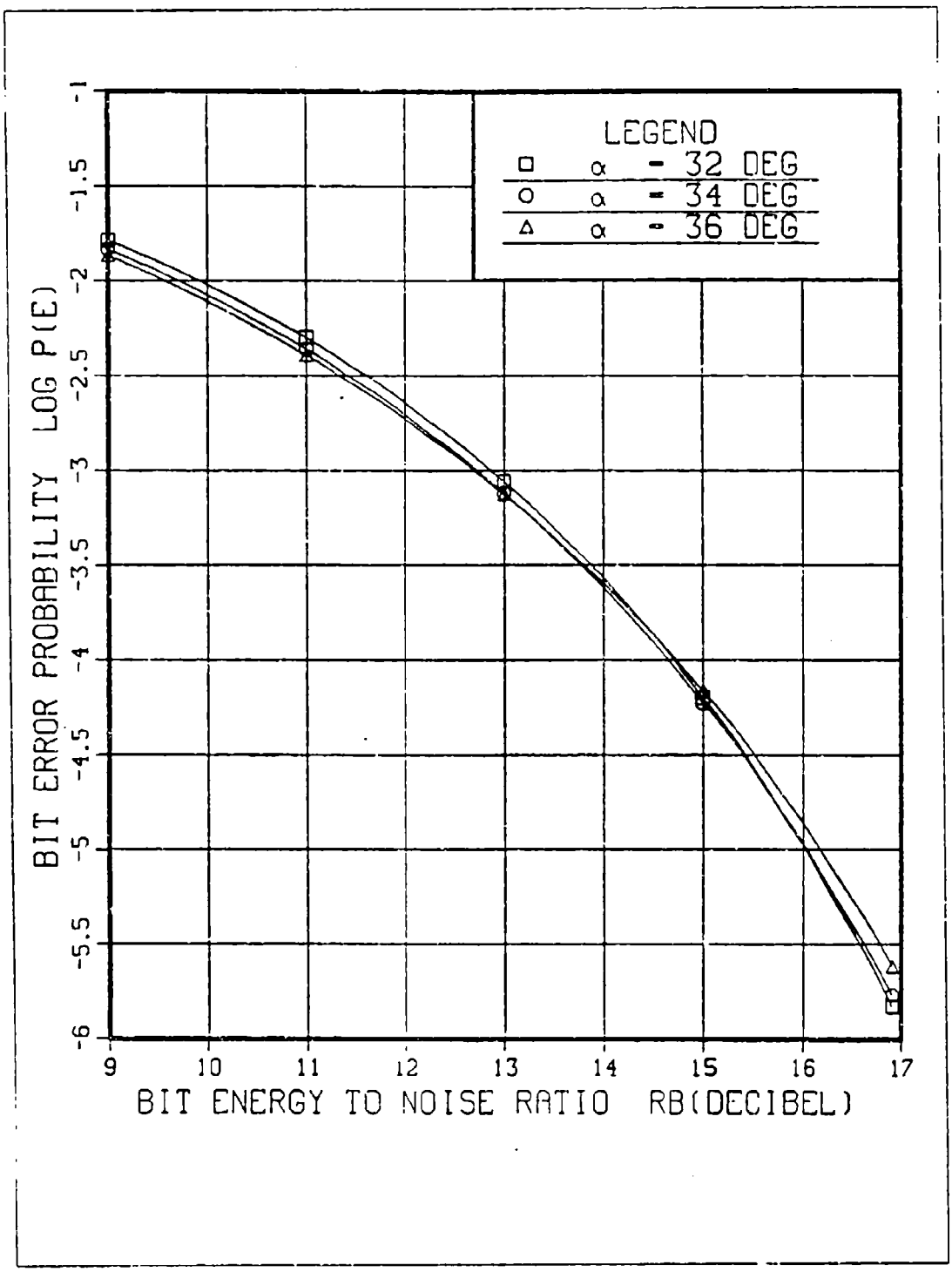

Figure 3.2 (b) Bit error probabilities for 8-PSK with bit detection receiver $\alpha = 32^{\circ} - 36^{\circ}$

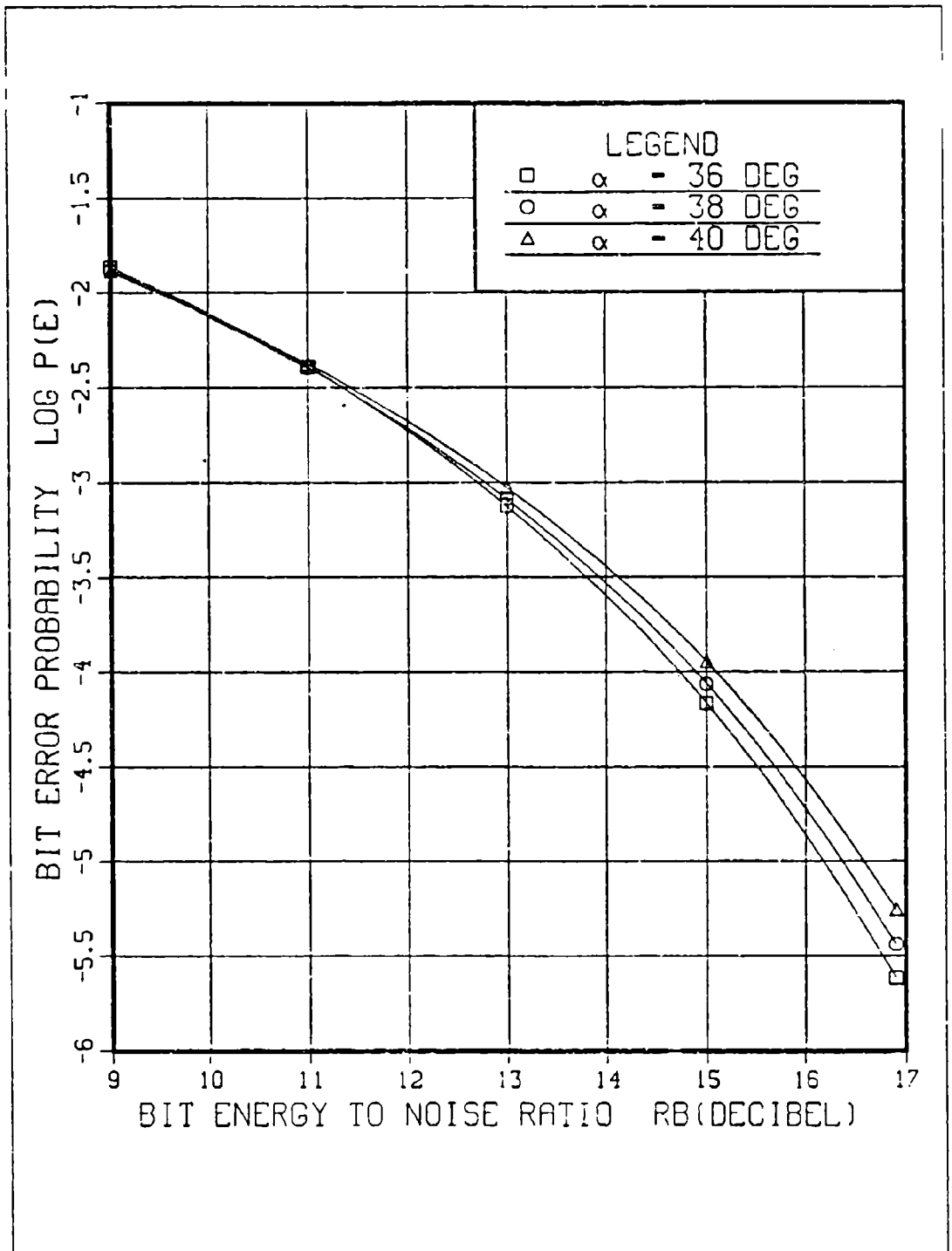

Figure 3.2 (c) Bit error probabilities for 8-PSK with bit detection receiver $\alpha = 36^{\circ} - 40^{\circ}$

Choosing an angle $\alpha = 32^{\circ}$, the bit error rate is computed and plotted alongside the bit error probability derived in Eqn. 2.29 for a standard phase detection receiver as described in Chapter 2. The results are shown in Figure 3.3. At a desired $P_b(E)$ of 10^{-5}, the bit detection receiver is seen to be 3 dB worse in bit energy-to-noise ratio compared with the standard phase detection receiver. The 3 dB represents a significant loss in performance. Moreover, the receiver requires a threshold setting of E/2 for the middle bit which is signal energy dependent and requires an automatic gain control (AGC) circuit for system adaptation so that a search for a better receiver is justified.

An alternate receiver structure is described in the following section whereby the same theoretical bit error rate of the standard phase receiver can be achieved with direct bit detection and at the same time allowing for a simplification in implementation in that only zero value thresholds are required so that there is no need for a AGC circuit.

B. MODIFIED BIT DETECTION RECEIVER FOR 8-PSK

The receiver structure presented in the previous section was modified slightly to obtain an improvement in bit error rate performance. The modified receiver structure is shown in Figure 3.4 whereby the modification involved only a change in the detection method of the middle bit. The middle bit is obtained by evaluating $(Y_1^2 - Y_2^2)$ and comparing this value to a zero threshold. This method is preferable also from the point of view that the receiver uses the thresholds that are signal energy independent. This is important because it eliminates the need for system adaptation and the use of automatic gain devices.

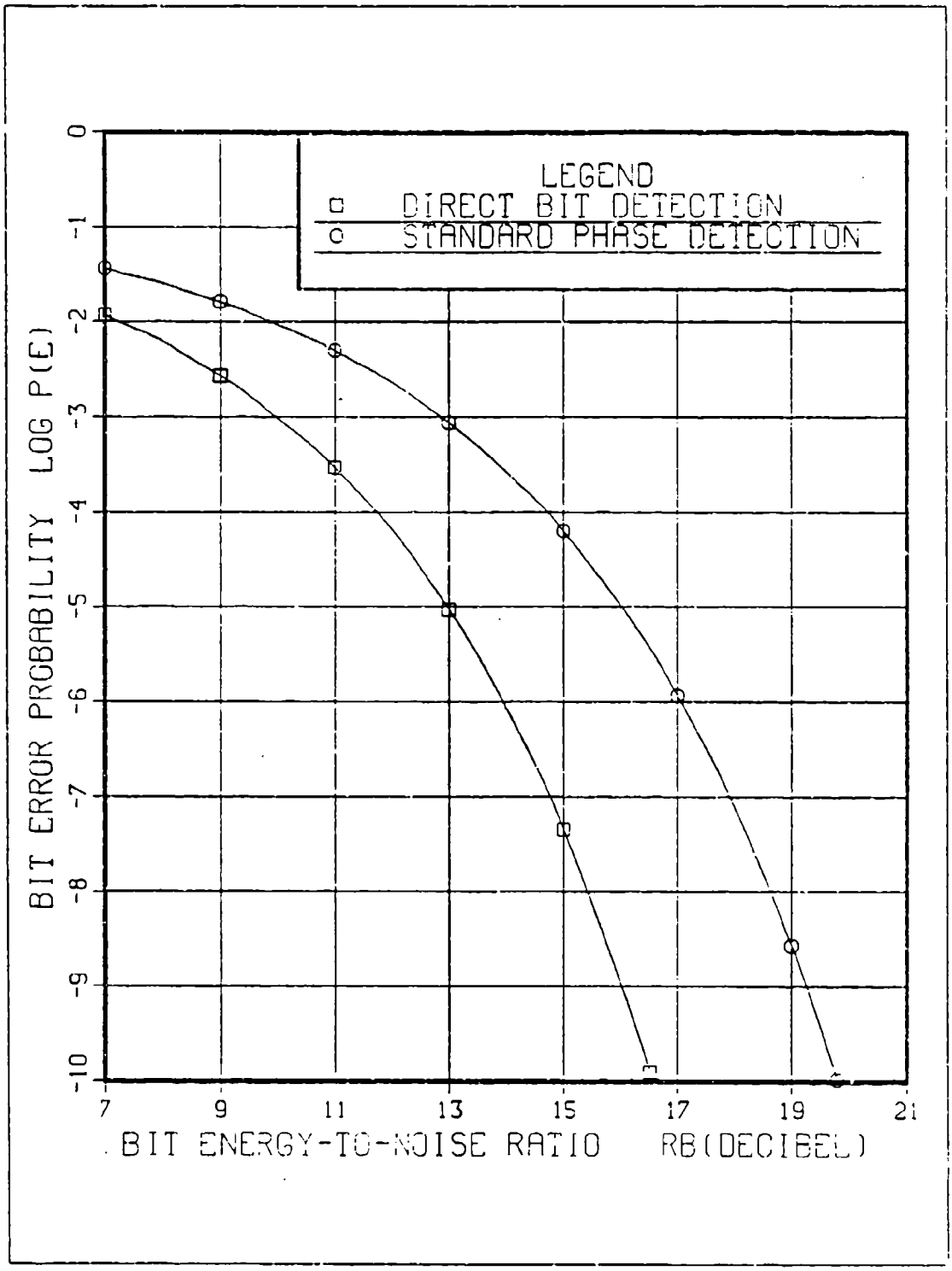

Figure 3.3 Bit error rate comparison of 8-PSK receivers using bit and phase detection methods

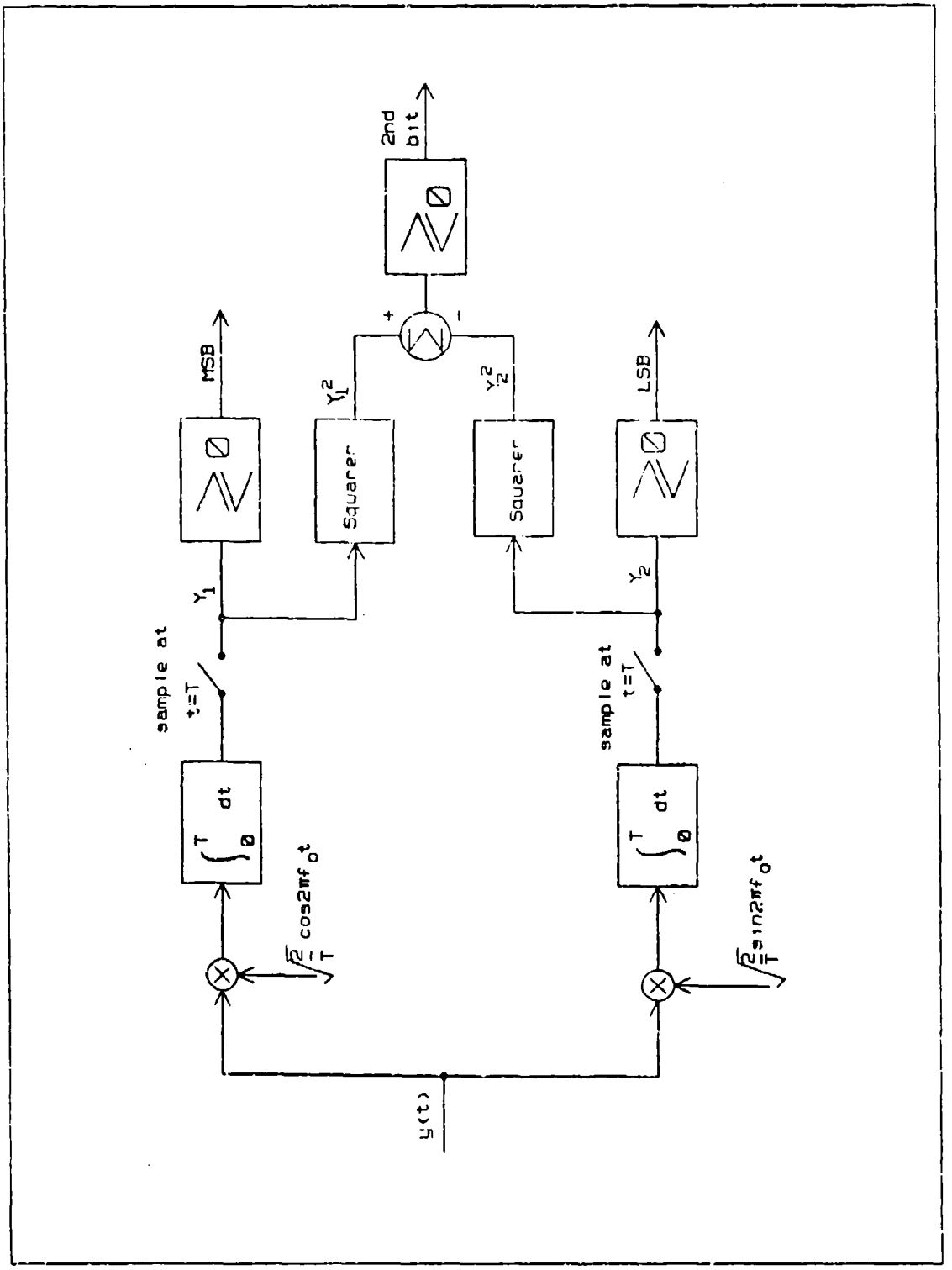

Figure 3.4 Modified bit detection receiver for 8-PSK

The error probability associated with middle bit is now determined by first obtaining the conditional pdf of $(Y_1^2 - Y_2^2) = \cos 2\eta$. Conditioned on $s_1(t)$ transmitted, correct decoding of the middle bit occurs when the received signal has positive values for $\cos 2\eta$. This implies a zero value threshold for the middle bit instead of E/2. Since $-\pi \leq \eta \leq \pi$,

$$\Pr\{\text{middle bit correct} | s_1(t) \text{ transmitted}\} = \Pr\{\cos 2\eta \geq 0\}$$

$$= \Pr\{-\pi/4 \leq \eta \leq \pi/4\} + \Pr\{-\pi \leq \eta \leq -3\pi/4\} + \Pr\{3\pi/4 \leq \eta \leq \pi\} \qquad \text{(eqn 3.4)}$$

Therefore the error probability for the middle bit can be derived by computing the pdf of η, the phase angle of the received signal vector. The derivation of the pdf of η can be found in [Ref. 4] where

$$p(\eta | s_i(t)) = \frac{e^{-d}}{2\pi}\left[1 + \sqrt{4\pi d}\cos\eta' \cdot e^{d\cos^2\eta'} \cdot Q\left(-\sqrt{d}\cos\eta'\right)\right]; \quad -\pi \leq \eta \leq \pi \qquad \text{(eqn 3.5)}$$

$$= 0 \; ; \quad \text{otherwise}$$

where $\eta' = \eta - \theta_i$

θ_i = phase angle of signal vector s_i

$d = E_s/N_o = 3E_b/N_o$ for 8-PSK.

Using the properties of rotational symmetry and equiprobable signals,

$$\Pr\{\text{middle bit correct} | s_i(t) \text{ transmitted}\} = \Pr\{\text{middle bit correct}\} \text{ for any } i \qquad \text{(eqn 3.6)}$$

$$= \int_{-\pi/4}^{\pi/4} p(\eta|s_1(t))d\eta + \int_{-\pi}^{-3\pi/4} p(\eta|s_1(t))d\eta + \int_{3\pi/4}^{\pi} p(\eta|s_1(t))d\eta$$

The above integrals can be evaluated numerically on a computer. It was found that for $E_b/N_o \geq 5$ dB, the contribution from the last two integrals is insignificant even when using double precision computation. Therefore

$$\Pr\{\text{middle bit error}\} = p_{ei} \qquad \text{(eqn 3.7)}$$

$$= 1 - \int_{-\pi/4}^{\pi/4} p(\eta|s_1(t))d\eta$$

so that

$$P_b(8) = 2p_{em}/3 + p_{ei}/3 \qquad \text{(eqn 3.8)}$$

For the modified receiver structure of Figure 3.4 , it was found that the optimum performance occurred with equal angle spacing between signals, ie $\alpha = 45^o$ and that at this optimum angle spacing, the bit error rate equals to those obtained for a standard phase detection receiver. This is a *significant result* in that similar performance can be achieved using simpler hardware structure and at the same time providing for direct and parallel bit decoding. This provides a potential for high speed data rate applications.

C. DIRECT BIT DETECTION FOR 16-PSK

The results obtained for the modified bit detection receiver when 8-PSK modulation is used, have provided motivation for the proposal of a bit detection receiver for 16-PSK modulation. The receiver and the signal constellation with bit code assignments are shown in Figure 3.5. Again only zero value thresholds and simple arithmetic operation like multiplication and subtraction are needed.

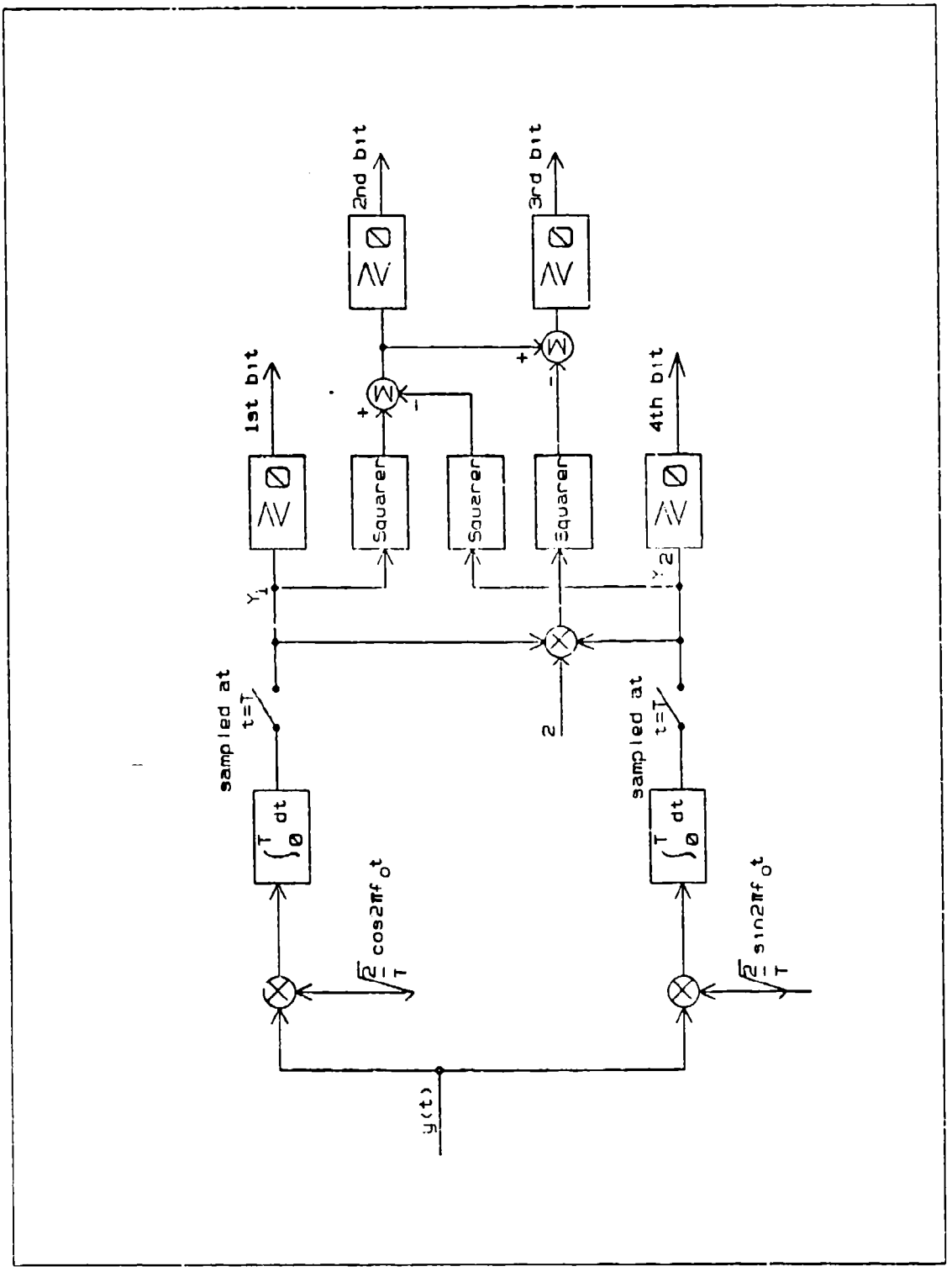

Figure 3.5 (a) Receiver structure for direct bit detection of 16-FSK

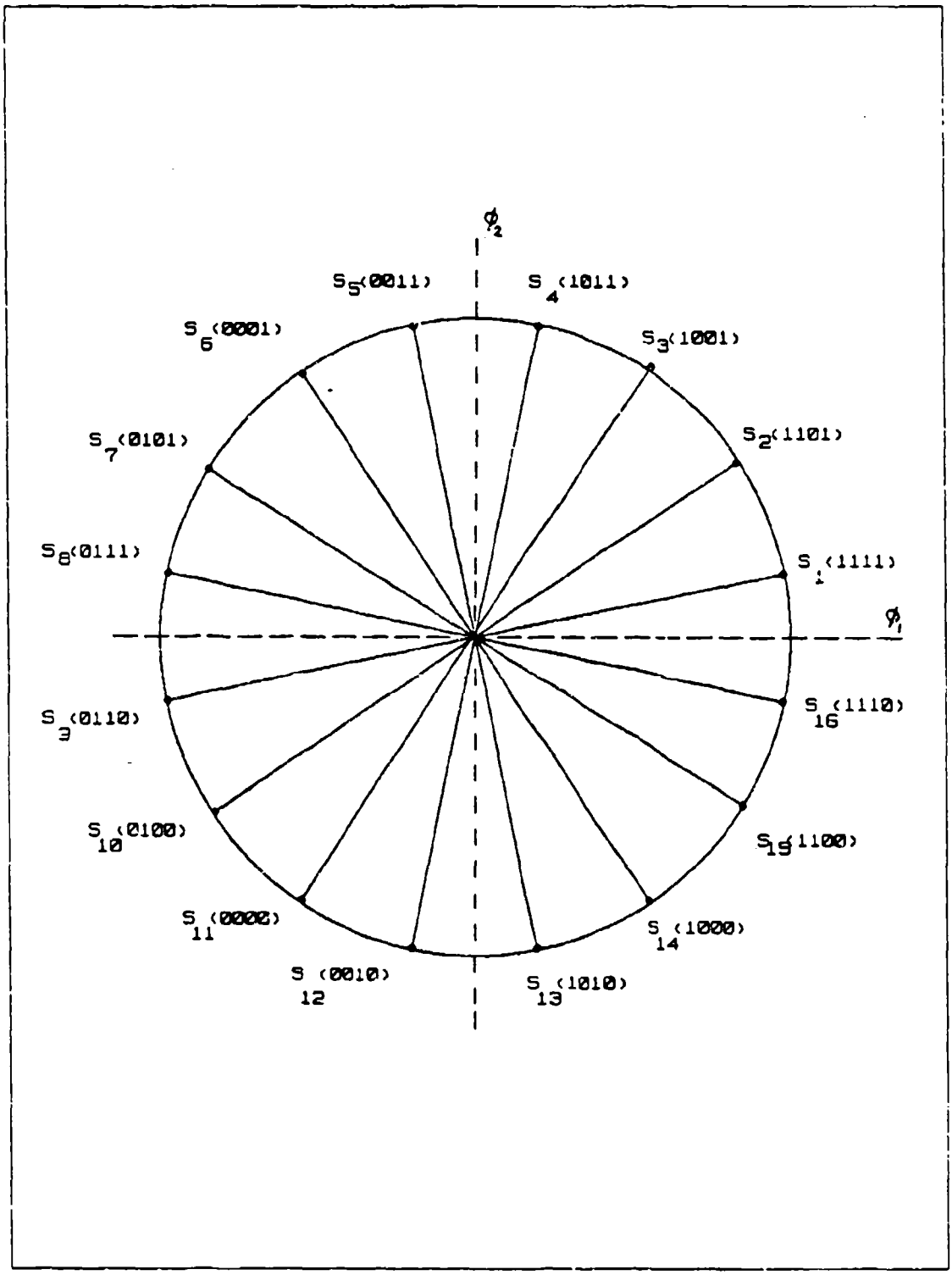

Figure 3.5 (b) Signal constellation and code assignment for 16-PSK with arbitrary phase angle spacing

Decisions for the first and last bits are based on the components of the received vector along the φ_1 and φ_2 axes, i.e., Y_1 and Y_2 respectively. Decision for the second bit is based on the value of $(Y_1^2 - Y_2^2) = \cos 2\eta$ in comparison to a zero threshold. The decision for the third bit can be obtained by evaluating the value of $\cos 4\eta$ and compared with a zero threshold. From the above description of the detection mechanism, the bit error performance is next derived. Define

p_{e1} = Pr{1st bit error}

p_{e2} = Pr{2nd bit error}

p_{e3} = Pr{3rd bit error}

p_{e4} = Pr{4th bit error}

Using the properties of rotational symmetry of signal vectors and equiprobable signals, p_{e1} can be obtained by considering only the four cases conditioned on $s_1(t)$, $s_2(t)$, $s_3(t)$, and $s_4(t)$ being transmitted, i.e.,

$$p_{e1} = 0.25[\ \Pr\{1\text{st bit error}|s_1(t)\} + \Pr\{1\text{st bit error}|s_2(t)\} + \Pr\{1\text{st bit error}|s_3(t)\} + \Pr\{\text{error}|s_4(t)\}\ ]$$

Following a similar analysis as was carried out in Eqn. 3.1 for 8-PSK, it can be seen that

$$p_{e1} = p_{e4} = 0.25[\ Q(\sqrt{2E/N_o}\sin\alpha) + Q(\sqrt{2E/N_o}\cos\alpha) + Q(\sqrt{2E/N_o}\sin\beta) + Q(\sqrt{2E/N_o}\cos\beta)]$$

For the 2nd bit, the decision is based on the parameter $(Y_1^2 - Y_2^2) = \cos 2\eta$ where η is the received signal vector's phase angle. The pdf of η conditioned on $s_i(t)$ transmitted is given by

$$p(\eta|s_i(t)) = \frac{e^{-d}}{2\pi}\left[1 + \sqrt{4\pi d}\cos\eta' . e^{d\cos^2\eta'} . Q\left(-\sqrt{d}\cos\eta'\right)\right];$$

$$-\pi \leq \eta \leq \pi \qquad \text{(eqn 3.9)}$$

$$= 0 \; ; \; otherwise$$

where $\eta' = \eta - \theta_i$

θ_i = phase angle of signal $s_i(t)$

$d = E_s/N_o = 4E_b/N_o$ for 16-PSK

Using the properties of rotational symmetry and equiprobable signals, it can be seen that p_{e2} can be obtained by considering only the two cases conditioned on $s_1(t)$ and $s_2(t)$ transmitted. Therefore

$$\Pr\{\text{2nd bit correct}\} = 0.5[\Pr\{\text{2nd bit correct}|s_1(t)\} + \Pr\{\text{2nd bit correct}|s_2(t)\}]$$

$$p_{e2} = 1 - 0.5\left[\int_{-\pi/4}^{\pi/4} p(\eta|s_1(t))d\eta + \int_{-\pi/4}^{\pi/4} p(\eta|s_2(t))d\eta\right] \qquad \text{(eqn 3.10)}$$

In Eqn. 3.6, the insignificant contributions from the integration of $p(\eta|s_1(t))$ and $p(\eta|s_2(t))$ over $[-\pi , -3\pi/4]$ and $[3\pi/4 , \pi]$ have been left out. For the decision on the third bit, the value of $\cos 4\eta$ was computed and compared to a zero value threshold. A bit value of 1's is assigned if $\cos 4\eta \geq 0$ and this happens when η falls in the following regions:

$[-\pi,-7\pi/8]$, $[-5\pi/8,-3\pi/8]$,

$[-\pi/8,\pi/8.]$, $[3\pi/8,5\pi/8]$, $[7\pi/8,\pi]$

Using the properties of rotational symmetry and equiprobable signals again, we obtained

$$p_{e3} = 1 - \Pr\{-5\pi/8 \leq \eta|s_1(t) \leq -3\pi/8\} - \Pr\{-\pi/8 \leq \eta|s_1(t) \leq \pi/8\} - \Pr\{3\pi/8 \leq \eta|s_1(t) \leq 5\pi/8\} \qquad \text{(eqn 3.11)}$$

whereby the insignificant contribution from the integration of $p(\eta|s_1(t))$ over the range $[-\pi,-7\pi/8]$ and $[7\pi/8,\pi]$ has been left out. The bit error probability is then given by

$$P_b(16) = p_{e1}/2 + p_{e3}/4 + p_{e4}/4 \qquad \text{(eqn 3.12)}$$

Numerical evaluations of the bit error probabilities were obtained with the aid of a computer. Again, it was found that optimum performance occurred at equal phase angle spacing between signals. The plot of bit error rate versus bit energy-to-noise ratio is shown in Figure 3.6 for the case of equal angle spacing ($\alpha = 11.25^{\circ}$) and also for unequal angle spacing where $\alpha = 10^{\circ}$. In the latter case, a loss of 1 dB signal-to-noise at $P_b(E) = 10^{-6}$ was incurred. The bit error rate for the case of equal angle spacing between signals agrees with that derived for a 16-PSK modulation standard phase detection receiver. This result together with the result obtained for a 8-PSK modulation suggest that for any M-ary PSK signal, it is likely that a direct bit detection receiver will always exist, having a theoretical bit error rate performance that is similar to that of a standard phase detection receiver. By carefully structuring the receiver, we can obtain parallel decoding of bits and also simplification in the hardware implementation. This result is important considering the present trend of using higher order modulation techniques due to the ever increasing demand for higher data rates in all forms of information transmission.

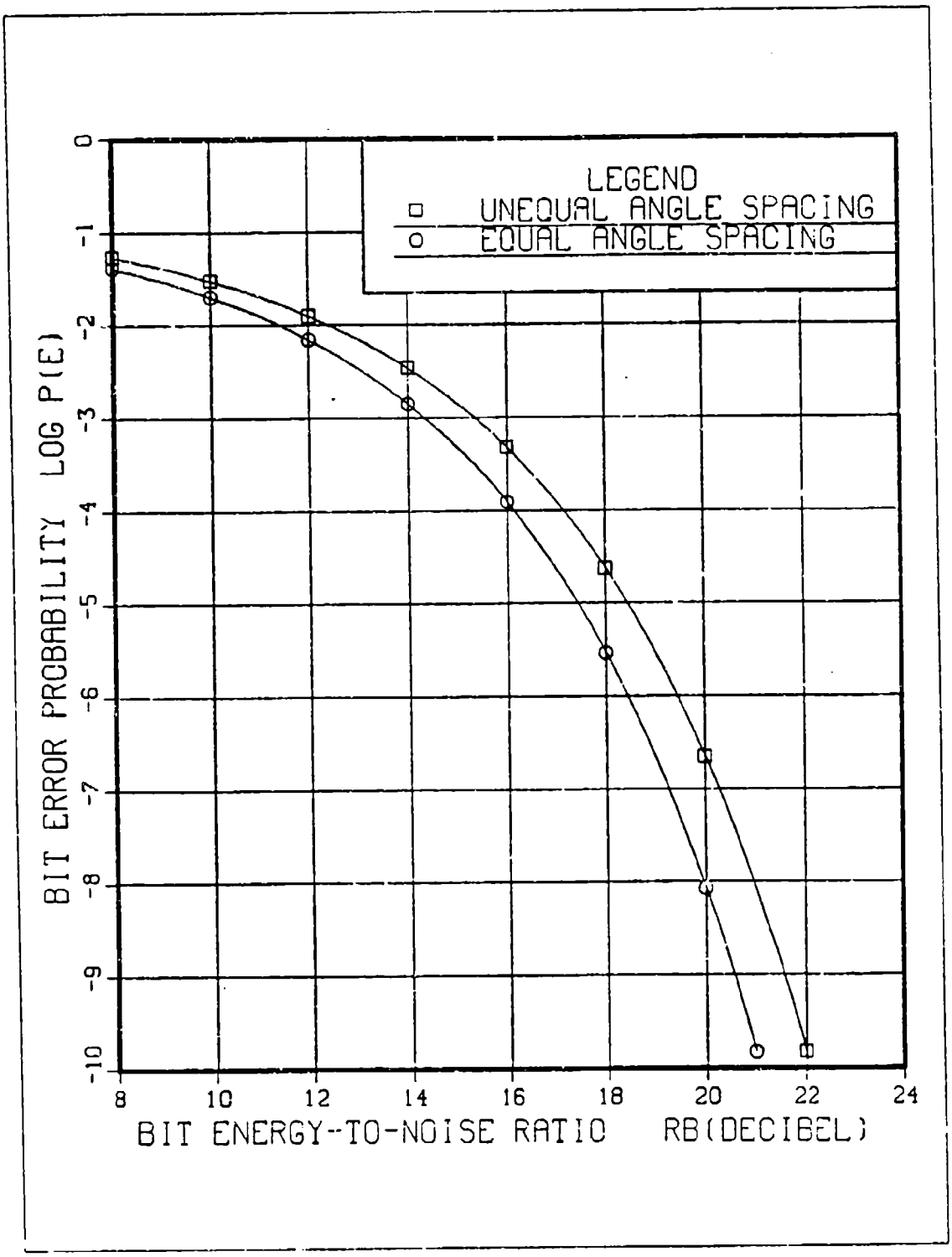

Figure 3.6 Performance of 16-PSK bit detection receiver with equal and unequal angle spacing

IV. FORWARD ERROR CORRECTION CODES

There are two different types of codes in common use today, namely block codes, and convolutional codes. In block coding, a sequence of bits is generated by a binary source which are then grouped into blocks of k bits long. To each of these k-bit blocks, (n-k) redundant symbols are are added to produce an n-symbol codeword. The (n-k) redundant symbols are referred to as the parity symbols. The result is denoted as an (n,k) block code. Since each codeword contains n symbols and conveys k bits of information, the information rate of the encoder output is k/n bits per symbol. This ratio k/n is also referred to as the code rate.

The encoder for a convolutional code also accepts k-bit blocks of information, and produces an encoded sequence of n-bit codewords. However, each codeword depends not only on the corresponding k-bit message block at the same time unit, but also on m previous message blocks. Hence, the encoder has a memory of order m. The set of encoded sequence produced by a k-input, n-output encoder of memory order m is called an (n,k,m) convolutional code. The ratio R = k/n is also the code rate as before. Since the encoder has memory, it must be implemented with sequential logic circuit.

A. SINGLE ERROR CORRECTING HAMMING BLOCK CODE

The single error correcting Hamming code form a class of block code which is known as perfect code in that all single errors and no other are correctable. For any positive integer $m \geq 3$, there exists a Hamming code with the following parameters:

Code length :	$n = 2^m - 1$
Number of information symbols:	$k = 2^m - m - 1$
Number of parity-check symbols:	$(n-k) = m$

Error correcting capability: t = 1(i.e. single error correction)

From the development of [Ref. 5 : pp. 79-81], the undetected codeword error probability of an (n,k) Hamming code is given by

$$P_u(E) = 2^{-m}\{1+(2^m-1)(1-2p)^{2^{m-1}}\} - (1-p)^{2^m-1} \qquad \text{(eqn 4.1)}$$

where m = n-k and p is the transitional probability of the binary symmetric channel (BSC) with additive white Gaussian noise interference.

For a (7,4) Hamming code, m = 3 so that

$$P_u(E) = 0.125\{1 + 7(1-2p)^4\} - (1-p)^7 \qquad \text{(eqn 4.2)}$$

Comparisons of coded and uncoded bit error rate performance must be done on an equitable basis. One way to do this is to require an equal transmitted message rate for both the coded and uncoded systems. For an encoded n-symbol codeword, the symbol energy is reduced somewhat because of the shorter bit duration when compared to the bit duration of the uncoded message sequence. Consider a k-bit message block encoded into an n-bit symbol block for transmission. The average symbol energy in the encoded sequence is reduced to

$$E_b' = kE_b/n$$

where E_b is the bit energy of the original uncoded message sequence.

1. Codeword error and bit error probabilities

The exact relationship between the codeword error probability of the transmitted sequence and the bit error probability of the message sequence is generally complicated and depends on the method used to generate the n-symbol from

the k-bit. Most references (see [Ref. 6] for example) compute upper and lower bounds or derive approximations to decoded bit error rate relationships based on high signal-to-noise assumptions. For an (n,k) code, if Γ denotes the average number of message bits in error for each codeword error, the bit error probability is given by

$$P_b(E) = \Gamma P_u(E)/k \qquad \text{(eqn 4.3)}$$

which is simply the ratio of the number of message bits in error to the total number of symbols in the codeword. The worst case occurs when each undetected codeword error results in k message bit error. This yield the simple upper bound

$$P_b(E) < P_u(E) \qquad \text{(eqn 4.4)}$$

The lower bound is obtained by considering the most favorable situation in which each undetected codeword error results in only one message bit error. For this case, Γ = 1, and

$$P_b(E) > P_u(E)/k \qquad \text{(eqn 4.5)}$$

For a perfect code with t-bit error correcting capability and if the signal-to-noise ratio is sufficiently high, the undetected error is most likely due to (t+1) bit errors in the codeword. Of these (t+1) bit errors in the codeword, (t+1)k/n are, on the average, message bit errors. Thus

$$\Gamma = (t+1)k/n \qquad \text{(eqn 4.6)}$$

and the approximation

$$P_b(E) = (t+1)P_u(E)/n \qquad \text{(eqn 4.7)}$$

result. The exact value of $P_b(E)$ for the (7,4) Hamming code will be derived next and compared with this approximation.

2. Bit error probability for (7,4) Hamming code

A (7,4) Hamming code can be generated using the generator polynomial $g(X) = 1+X+X^3$ The message blocks and the corresponding codewords are shown in Table 2 below.

TABLE 2

A (7,4) HAMMING CODE GENERATED BY $G(X) = 1+X+X^3$

Message	Codeword
0000	0000 000
1000	1101 000
0100	0110 100
1100	1011 100
0010	1110 010
1010	0011 010
0110	1000 110
1110	0101 110
0001	1010 001
1001	0111 001
0101	1100 101
1101	0001 101
0011	0100 011
1011	1001 011
0111	0010 111
1111	1111 111

The standard array is next constructed and shown in Table 3. The seven correctable single error patterns and the all zero pattern are used to form the first elements in each column and the sixteen valid codewords are used to form the first elements in each row of the standard array.

TABLE 3

STANDARD ARRAY FOR (7,4) HAMMING CODE

code-word	coset leader------->						
0000000	1000000	0100000	0010000	0001000	0000100	0000010	0000001
1101000	0101000	1001000	1111000	1100000	1101100	1101010	1101001
0110100	1110100	0010100	0100100	0111100	0110000	0110110	0110101
1011100	0011100	1111100	1001100	1010100	1011000	1011110	1011101
1110010	0110010	1010010	1100010	1111010	1110110	1110000	1110011
0011010	1011010	0111010	0001010	0010010	0011110	0011000	0011011
1000110	0000110	1100110	1010110	1001110	1000010	1000100	1000111
0101110	1101110	0001110	0111110	0100110	0101010	0101100	0101111
1010001	0010001	1110001	1000001	1011001	1010101	1010011	0101111
0110110	1111001	0011001	0101001	0110001	0111101	0111011	0111000
1100101	0100101	1000101	1110101	1101101	1100001	1100111	1100100
0001101	1001101	0101101	0011101	0000101	0001001	0001111	0001100
0100011	1100011	0000011	0110011	0101011	0100111	0100001	0100010
1001011	0001011	1101011	1011011	1000011	1001111	1001001	1001010
0010111	1010111	0110111	0000111	0011111	0010011	0010101	0010110
1111111	0111111	1011111	1101111	1110111	1111011	1111101	1111110

The remaining elements in the array are generated as follows: let D_j denotes the jth column of the standard array. Then

$$D_j = \{ v_j, e_2+v_j, e_3+v_j, \ldots, e_8+v_j \}$$

where v_j is a valid codeword and $e_2, e_3, \ldots, e_8$ are the single error patterns known also as the coset leaders. Using these rules, the columns in the standard array of the (7,4) Hamming code are constructed and the array shown in Table 3. Suppose the codeword v_j is transmitted over a noisy channel. We see that the received codeword r is in D_j if the error pattern caused by the channel is a coset leader and hence will be decoded correctly into the codeword v_j.

Since the coset leaders are single error symbol patterns, undetected errors occur only when there are two or more symbol errors in the received symbol pattern. It can be shown that if the transitional probability p of the binary symmetric channel is in the order of 10^{-2} or less, the only significant contribution to the undetected error probability comes from the 2-symbol error patterns in the codeword. Based on this, an algorithm is devised in order to compute the average bit errors in the message block given that a 2-symbol error have occurred in the received codeword. The is done as follows: conditioned on each of the sixteen possible codewords, all 2-symbol error patterns are computed. These erroneous code patterns are then 'corrected' using the standard array into its corresponding coset leaders and then decoded into the corresponding message blocks. From this the average message bit error probability can be computed. This procedure is best illustrated with an example. Conditioned on the all zero codeword transmitted, the possible 2-symbol error codewords, the 'corrected' codewords of the coset leaders and the message blocks are

computed and is shown in Table 4. Of the 21 possibilities of double symbol errors in the received codeword, nine of them yield single bit errors while another nine result in 2-bit errors. The remaining three possibilities produce 3-bit errors in the message blocks.

The same computation of the bit error patterns were carried out for each of the other 15 codewords assumed to be transmitted. Similar results to those obtained for the case in which the all zero codeword was assumed transmitted were observed due to a property that Hamming codes possess that puts them in the class of so-called perfect codes. It is possible to conclude now that Γ, the average number of message bit error given that an undetected codeword error has occurred is given by

$$[(9x1) + (9x2) + (3x3)]/21 = 12/7$$

Therefore, the bit error rate in the message block for a (7,4) Hamming code is approximately given by

$$P_b(E) = \Gamma P_u(E)/k = 3P_u(E)/7 \qquad \text{(eqn 4.8)}$$

$$= 3[1+7(1-2p)^4]/56 - 3(1-p)^7/7$$

Comparing this result with Eqn. 4.7 which states that $P_b(E) = 2P_u(E)/7$, it can be seen that the approximation is off by a factor of 2/3 which is reasonably good for the simple estimate developed.

B. SINGLE ERROR CORRECTING AND DOUBLE ERROR DETECTING HAMMING CODE

The Hamming code is also a cyclic code in that every cyclic shift of any code vector results in another valid code vector. The cyclic Hamming code can be modified so as to be able to correct any single error and simultaneously detect any combination of double errors.

TABLE 4

COMPUTATION OF AVERAGE BIT ERROR IN MESSAGE BLOCK FOR A (7,4) HAMMING CODE

** Conditioned on codeword 0000000 transmitted

2-bit error codeword	Coset leader	Message block	# of bit error
0101000 1001000 1100000	1101000	1000	1
0010100 0100100 0110000	0110100	0100	1
0001010 0010010 0011000	0011010	1010	2
0000110 1000010 1000100	1000110	0101	2
0010001 1000001 1010000	1010001	0001	1
0000101 0001001 0001100	0001101	1101	3
0100001 0000011 0100010	0100011	0011	2

In application where retransmissions are allowed and easily accomplished, this is definitely an added advantage. A single-error-correcting and double-error-detecting Hamming code of length 2^m-1 is generated by the polynomial

$$g(X) = (X+1)p(X) \qquad \text{(eqn 4.9)}$$

where p(X) is the primitive polynomial of degree m used to generate the single-error-correcting Hamming code. Note that this code has (m+1) parity check bits and is denoted as a (n,k-1) code.

Let C_1 and C_2 represent the single-error-correcting Hamming code and its corresponding modified code providing double-error-detection respectively. It can be shown [Ref. 5: pp. 113-114] that the minimum distance of code C_2 is 4. Also this distance 4 Hamming code C_2 consists of all the even weight code vectors of the corresponding distance 3 code C_1, and the undetected error probability of this code when transmission takes place over a BSC is given by [Ref 5: pp. 115-116],

$$P_u(E) = 2^{-(m+1)}\{1+2(2^m-1)(1-p)(1-2p)^{2^{m-1}-1}+(1-2p)^{2^m-1}\} - (1-p)^{2-1} \qquad \text{(eqn 4.10)}$$

where p is the transitional probability over the BSC channel.

For the (7,3) Hamming code C_2, the general formula above becomes (m = 3)

$$P_u(E) = 2^{-4}\{1+14(1-p)(1-2p)^3+(1-2p)^7\} - (1-p)^7 \qquad \text{(eqn 4.11)}$$

Following the same type of analysis as carried out in the previous section in order to compute the average message bit

error probability, a search for all possible 3-symbol errors in the received codeword is performed. The same standard array presented for the (7,4) Hamming code and shown in Table 3 can be used to correct the 3-symbol error codewords. Note that all the 3-symbol error patterns are always 'corrected' as a valid codeword (i.e. one with even weight). This is illustrated in Table 5 which shows all the possible 3-symbol error patterns and the corresponding coset leaders based on the assumption that the all zero codeword has been transmitted.

Since there are eight valid codewords in C_2, each codeword is assigned to a 3-bit message block. It can be seen from Table 5 that when a 3-bit error occurs, it is equally likely that any one of the seven remaining codewords is assigned. Hence there is no prefered way of assigning the message bits to the codeword so as to reduce the average bit error rate in the message block. The same results were obtained when the computation was carried out under the assumption of other codewords being transmitted. Therefore the average number of message bits in error given an undetected error has occurred is given by

$$\Gamma = [(3x1 + (3x2) + (1x3)]/7 = 12/7$$

which is identical to the previous result. The message bit error rate then becomes

$$P_b(E) = \Gamma P_u(E)/k = 4P_u(E)/7 \qquad \text{(eqn 4.12)}$$

$$= \{1+14(1-p)(1-2p)^3+(1-2p)^7\}/28 - 4(1-p)^7/7$$

The two different forms of the Hamming code are now applied to digital transmission via an optimum 16-PSK modulation channel in order to illustrate possible coding gains.

TABLE 5

COMPUTATION OF AVERAGE MESSAGE BIT ERROR
FOR A (7,3) DOUBLE-ERROR-DETECTING HAMMING CODE

** Conditioned on the codeword 0000000 transmitted

3-bit error patterns	coset leader
0011100 1001100 1010100 1011000	1011100
0110010 1010010 1100010 1110000	1110010
0001110 0100110 0101010 0101100	0101110
0011001 0101001 0110001 0111000	0111001
0100101 1000101 1100001 1100100	1100101
0001011 1000011 1001001 1001010	1001011
0000111 0010011 0010101 0010110	0010111

The comparisons between the coded and uncoded case were made assuming equal transmitted information rate so that the

symbol energy-to-noise ratio for the coded case is reduced by a factor of k/n. The performance associated with 8-PSK modulation was included for comparison purposes. Figure 4.1 shows the four curves of the bit error probabilities as follows:

(a) 16-PSK receiver without coding

(b) 16-PSK with (7,4) Hamming code

(c) 16-PSK with (7,3) single-error-correcting and double-error-detecting Hamming code

(d) 8-PSK receiver without coding

Figure 4.1 illustrates the superiority of channel coding especially when operating under weak signal-to-noise conditions. For example, if there is a constraint on E_b/N_o to be equal to or less than 9 dB, the results yield the following bit error rates (BER):

16-PSK without code :	BER = 3×10^{-2}	
16-PSK with (7,4) code:	BER = 5×10^{-4}	(decoded)
16-PSK with (7,3) code:	BER = 1×10^{-4}	(decoded)
8-PSK without code :	BER = 3×10^{-3}	

The reduction in BER is in the order of a factor of 10^2 with coding whereas the BER reduction obtained from reducing the order of modulation to 8-PSK is only in the order of a factor of 10. For high signal-to-noise ratio, the performance gain associated with 8-PSK is only 1 dB better than that of the coded 16-PSK. The above comparisons take into account the reduction in E_b/N_o inherent with coding so that equal information transmission rates in all cases are maintained without having to increase the transmitted power.

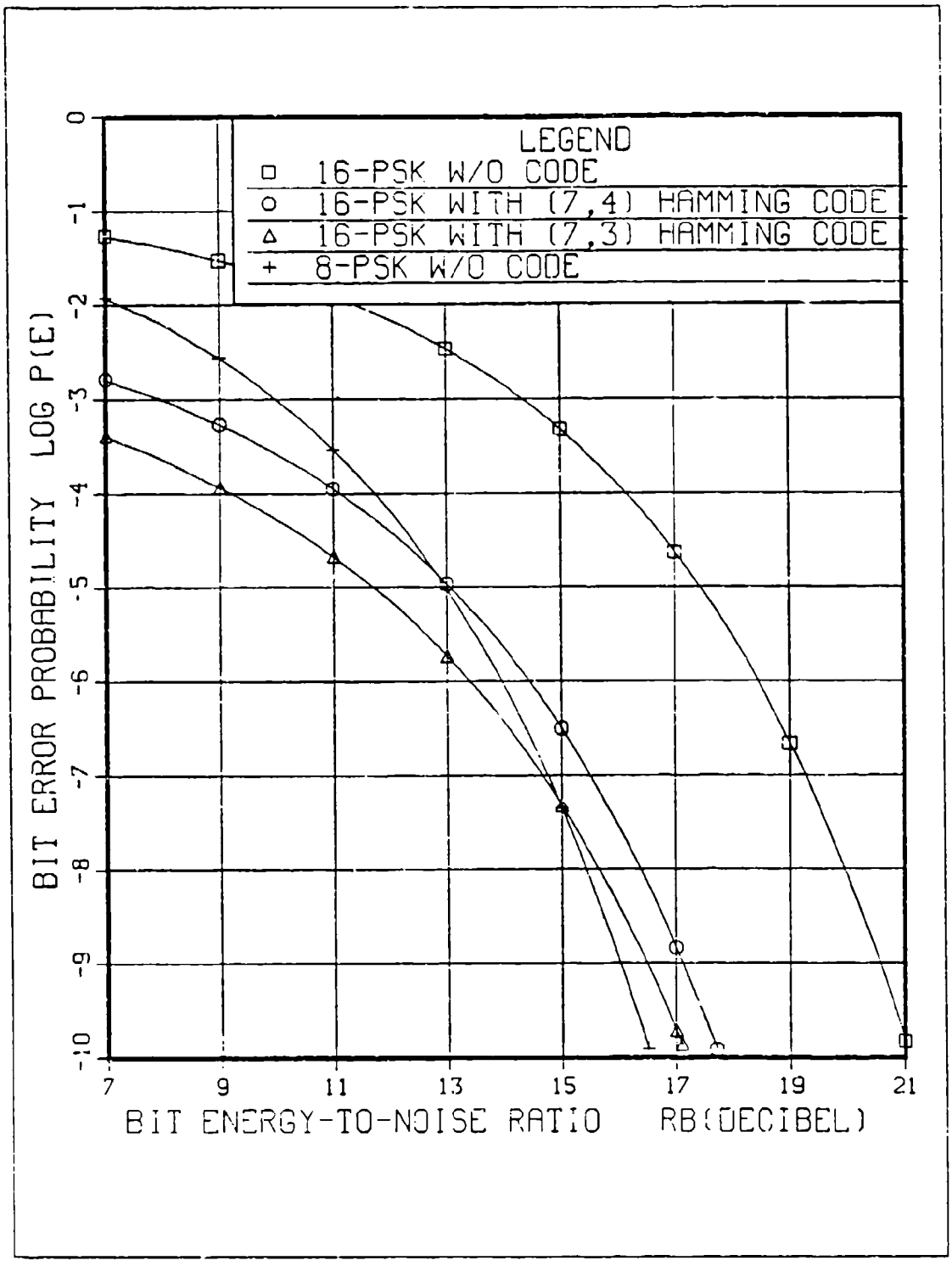

Figure 4.1 Bit error rate comparisons of 16-PSK with and without Hamming code

Another point worth noting is that for the (7,3) Hamming code, the performance is not significantly better than the (7,4) code even though the detected but non-correctable errors have not been included in the bit error calculation. Since the most likely errors in a typical communication system is due to single errors if Gray coding is used, the performance improvement from the use of double-error-detection codes is sometimes not significant. Furthermore, the need to implement a repeat request strategy makes the (7,3) Hamming code less popular than the (7,4) Hamming code. At a BER = 10^{-5}, the coding gain from the (7,4) Hamming code is about 4.5 dB which is also the crossover point beyond which the uncoded 8-PSK system yields superior performance.

C. CONVOLUTIONAL CODES

It is expected that convolutional codes will predominate in their application to space and satellite communication systems because such codes are relatively easy to implement and several attractive decoding schemes for high speed decoding exist and are available as "of the shelf" systems. The classic Viterbi decoding algorithm is an excellent example where the decoder implementation can be accomplished using sequential circuits that require only add, compare and select operations. In practice, at a bit error probability of 10^{-5}, a rate one-half code and a Viterbi decoder using soft decisions can easily reduce the required signal energy per bit by about 5 dB at the cost of bandwidth expansions of a factor of two as were be shown in the subsequent sections.

1. Convolutional encoders

A very important parameter in the design of a convolutional encoder which influences the performance of the code is the constraint length, L, which is defined as the number of encoder outputs that are affected by a single input message bit. If the encoder contains k banks of shift

registers, not all of which must be of the same length, then the encoder memory order, m, is defined as the maximum length of all the k banks of shift registers. The constraint length is then defined as

$$L = n(m+1)$$

Another important parameter which affects the memory size of the decoder is the total encoder memory, K, which is defined as

$$K = \sum_{i=1}^{k} K_i$$

where K_i is the length of the ith bank of shift registers.

To enable a fair comparison of the (7,4) Hamming code analyzed in the previous section, convolutional codes with total encoder memory, K = 4 were chosen in this section for analysis and comparisons. The rate one-half and the rate two-third codes were chosen as they possess code rates that are close to that of the (7,4) Hamming code. Therefore a (2,1,4) code and a (3,2,2) code were analyzed. The criteria for choosing the encoder structure is one that maximizes the free distance d_{free} of the code. From [Ref 5: p. 330], the best (2,1,4) code which gives the maximum d_{free} is obtained by utilizing the generating sequences

$$g^{(1)} = (1\ 0\ 0\ 1\ 1)$$

$$g^{(2)} = (1\ 1\ 1\ 0\ 1)$$

which gives $d_{free} = 7$. The encoder implementation of this code is shown in Figure 4.2.

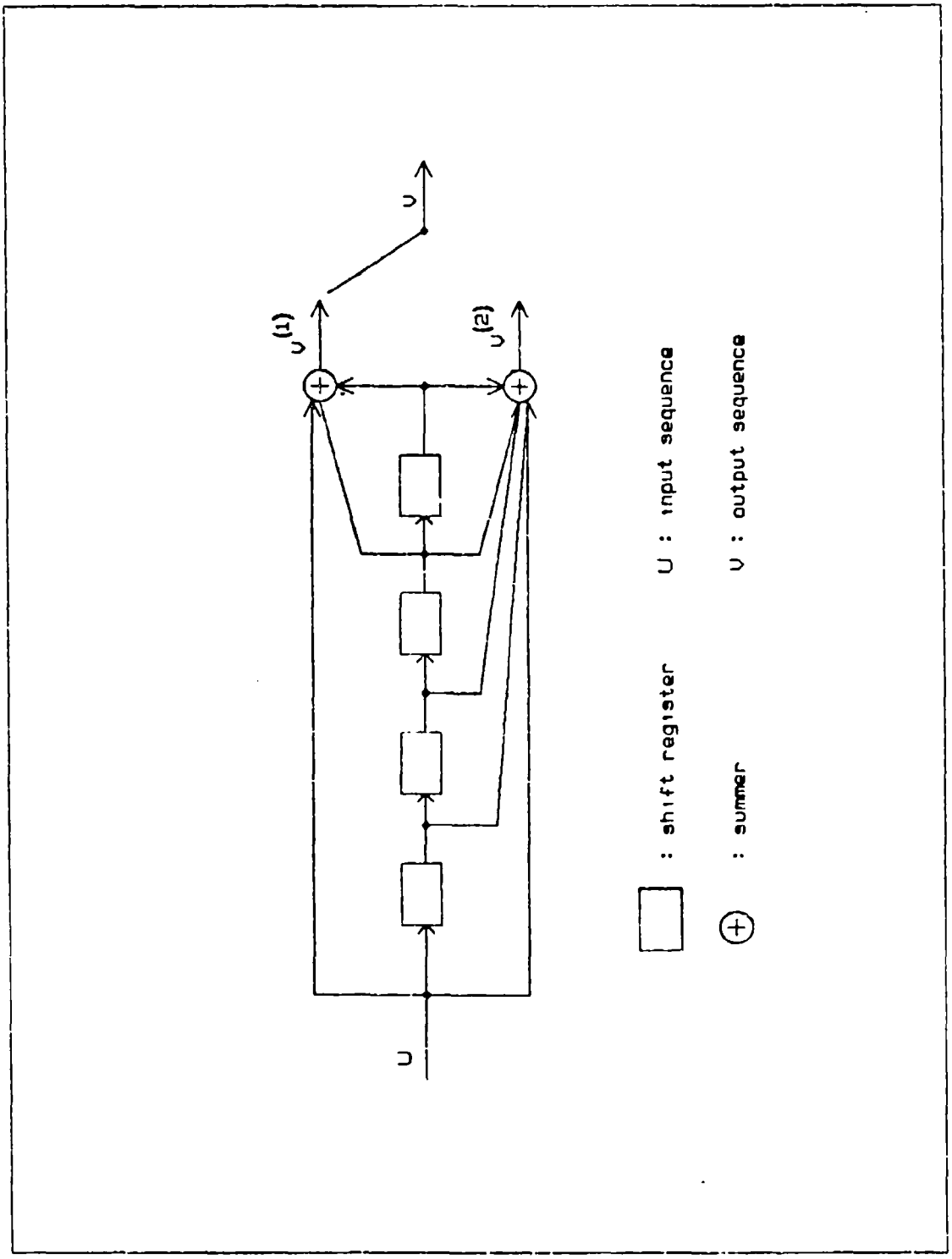

Figure 4.2 Encoder for (2,1,4) convolutional code with $d_{free} = 7$

The best (3,2,2) code is generated by the following sequences

$$g_1^{(1)} = (\ 1\ 1\ 1\ ) \qquad g_2^{(1)} = (\ 0\ 1\ 0\ )$$

$$g_1^{(2)} = (\ 0\ 0\ 1\ ) \qquad g_2^{(2)} = (\ 1\ 0\ 1\ )$$

$$g_1^{(3)} = (\ 1\ 0\ 0\ ) \qquad g_2^{(3)} = (\ 1\ 1\ 1\ )$$

and the corresponding encoder implementation is shown in Figure 4.3.

2. Viterbi decoding

The main advantage of Viterbi decoding algorithm lies with the relative ease of hardware implementation with which simple operations like add, compare and select are performed thus allowing for high speed digital implementation. This made it possible to operate at data rates in the order of megabit per second. From the development given in [Ref 5, pp. 322-328], it is shown that the decoded bit error rate using Viterbi decoding is given by

$$P_b(E) \simeq (B_{dfree}/k)(2\sqrt{p(1-p)}\ )^{dfree} \qquad \text{(eqn 4.13)}$$

where B_{dfree} is the number of paths with distance equal to d_{free} in the encoder state diagram and p is the transitional probability of the BSC. Since d_{free} of the chosen code is known, the problem now involves determining B_{dfree}. This is done by constructing a state diagram for the encoders as shown in Figures 4.4 and 4.5.

For the (2,1,4) code, it can be seen that $d_{free} = 7$ occurs for only one sequence, $s_0s_1s_2s_4s_8s_0$ so that $B_{dfree} = B_7 = 1$ and $P_b(E)$ from Eqn. 4.13 becomes

$$P_b(E) \simeq [\,2\sqrt{p(1-p)}\ ]^7 \qquad \text{(eqn 4.14)}$$

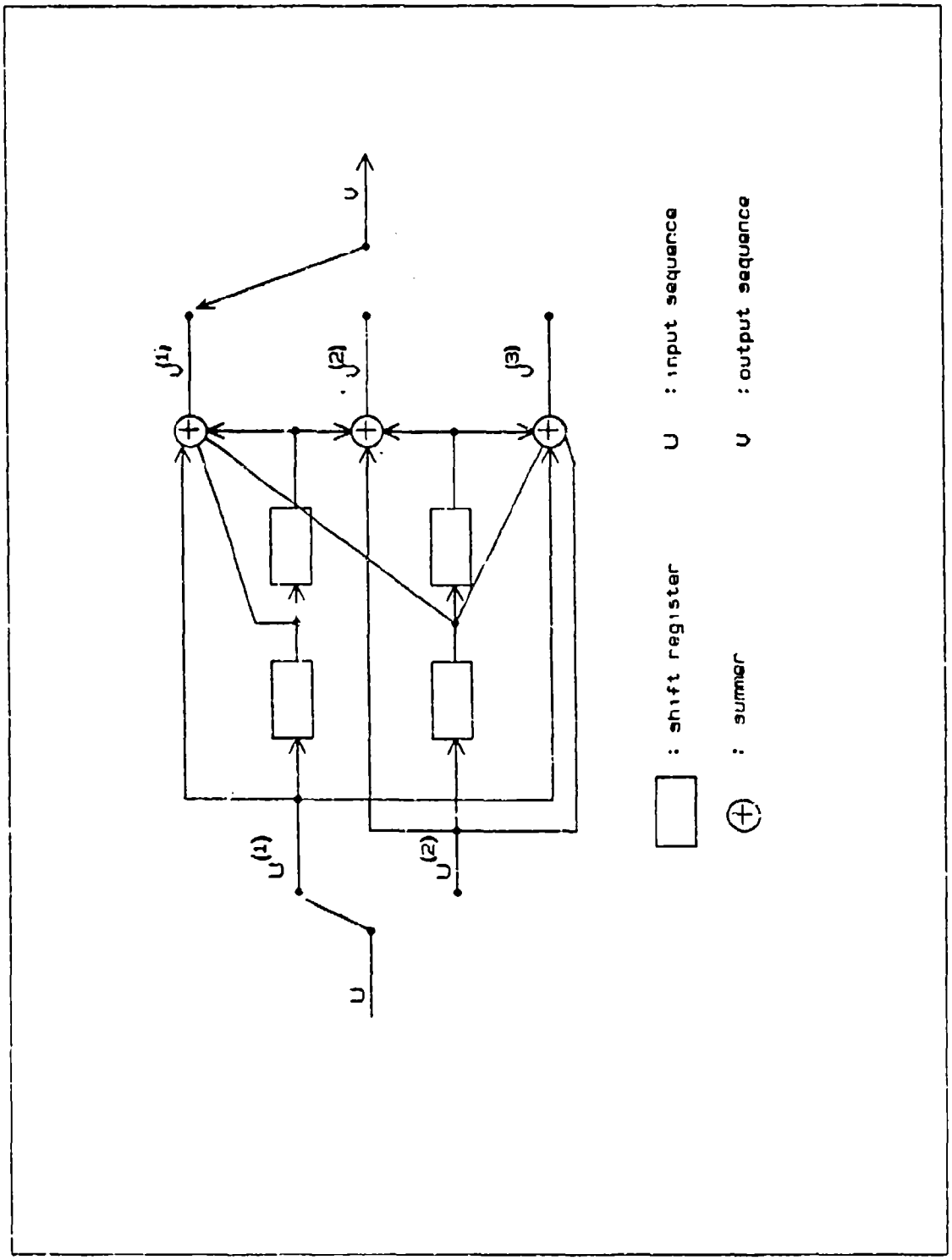

Figure 4.3 Encoder for (3,2,2) convolutional code with $d_{free} = 5$

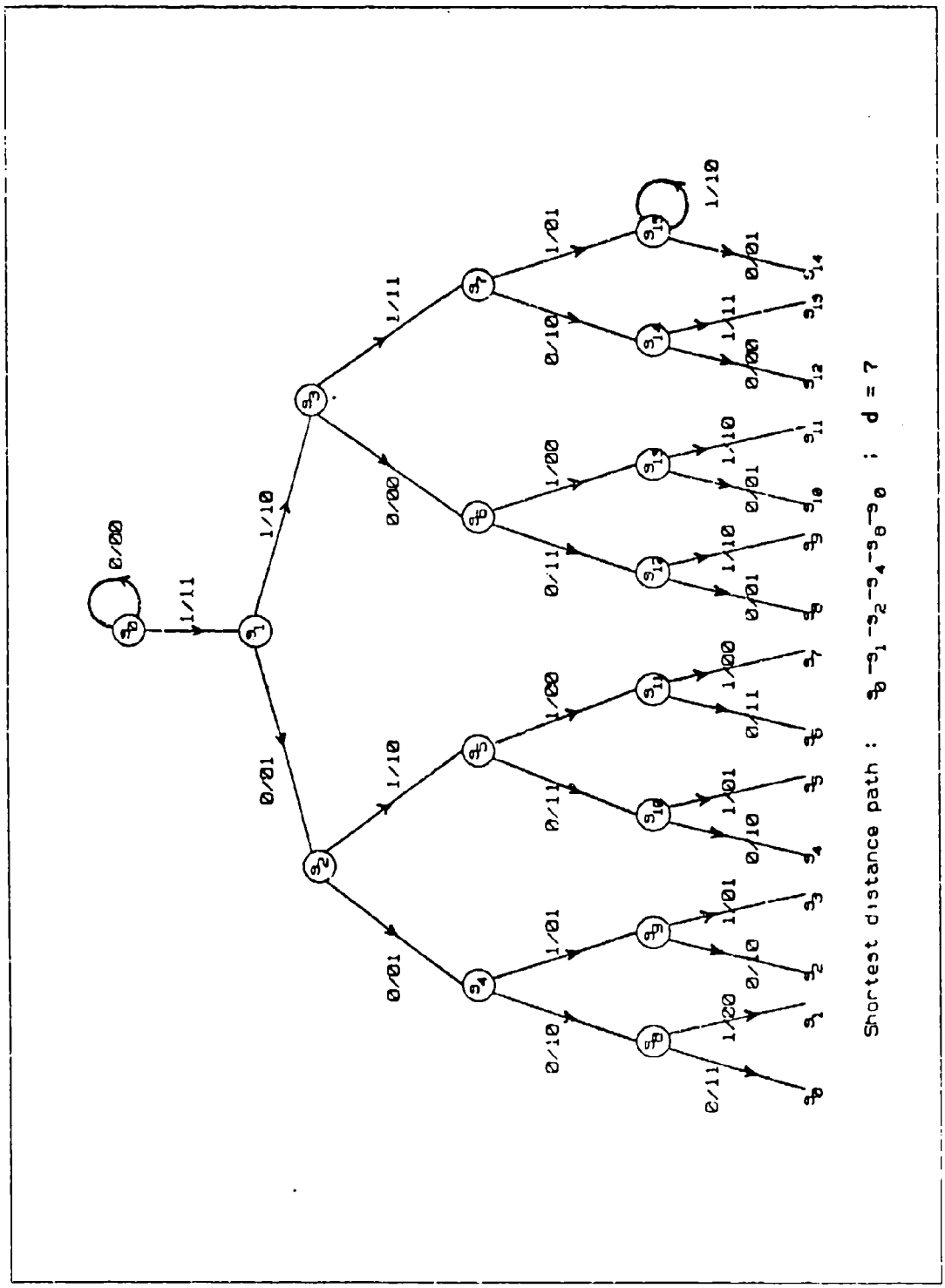

Figure 4.4 Encoder state diagram for (2,1,4) code

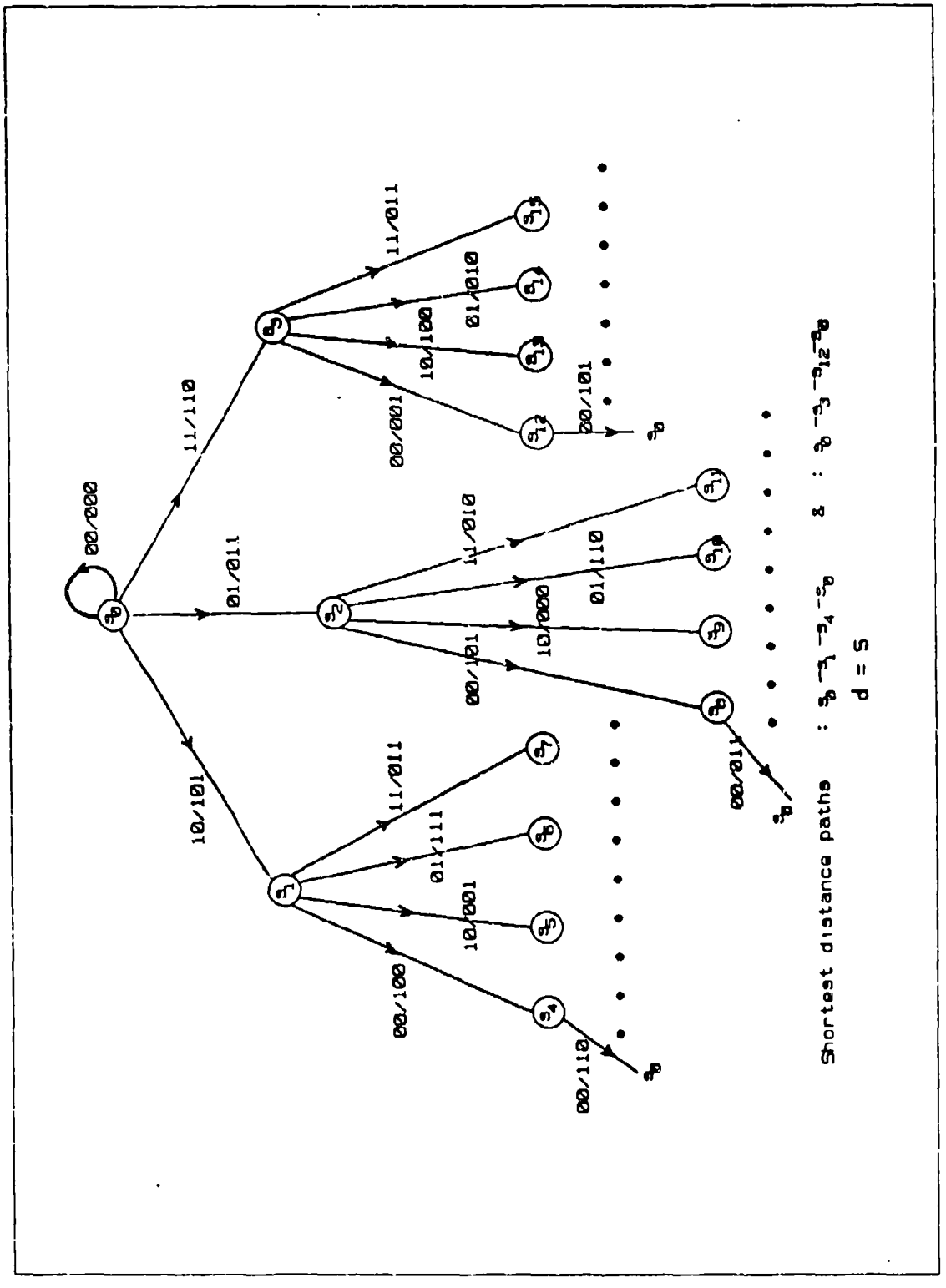

Figure 4.5 Encoder state diagram for (3,2,2) code

For the (3,2,2) code, it can be seen that $d_{free} = 5$ occurs for 2 paths: $s_0 s_1 s_4 s_0$ and $s_0 s_3 s_{12} s_0$ so that

$$P_b(E) \simeq [2\sqrt{p(1-p)}]^5 \qquad \text{(eqn 4.15)}$$

In order to enable a fair comparison of the different schemes considered based on equal transmitted information rates, the values of E_b/N_o were reduced by a factor of 1/2 and 2/3 respectively for the encoded symbols produced by the two encoders. Figure 4.6 shows the decoded bit error rate plots of the convolutionally coded data transmitted via 16-PSK modulation with Viterbi decoding using hard decisions (i.e. the output is quantized into only 2 levels). In order to improve the code performance, there are two possible modifications, namely

(a) Increase K, the total encoder memory of the code

(b) Use soft decisions instead of hard decisions, i.e. increase the number of quantization levels in the output beyond two.

Heller and Jacobs [Ref. 7] conducted extensive computer simulation studies on the performance of codes with different encoder memory size, K, and the number of output quantization levels, Q. It was found that the coding gain (improvement) obtained by increasing K from 4 to 5 was only about 0.5 dB. Furthermore, a decoder for a code of memory of order K, requires storage (memory) that is proportional to 2^K Therefore arbitrary increases in K without significant performance improvements are not practical. [Ref 5: p. 337]. In many cases, a value of K = 8 is considered the practical limit for the Viterbi algorithm. On the other hand increasing the output quantization levels from Q = 2 to Q = 8 requires a much smaller increase in memory size.

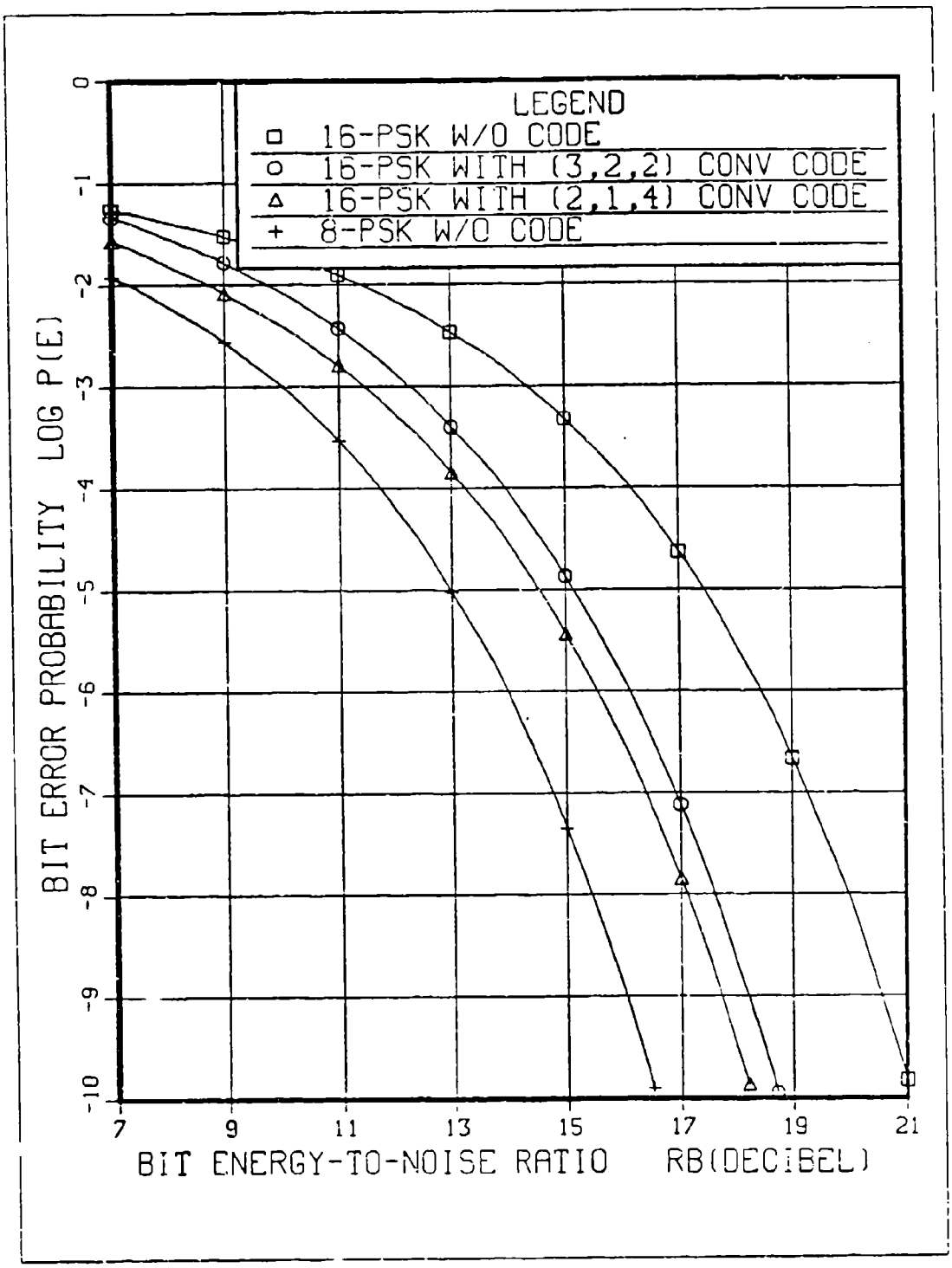

Figure 4.6 Bit error rates of 16-PSK with and without convolutional codes Q = 2

The performance improvement however can be shown to provide coding gains of about 1.7-2 dB over the range of interest for K = 4 and K = 5 codes. These improvements are illustrated in Figure 4.7 which shows that the performance gains of the two convolutional codes become comparable with that of the Hamming codes considered in the previous section. A theoretical proof [Ref. 8] shows that the performance gain from using infinitely fine quantization levels in soft decision decoding is 2 dB so that the use of Q = 8 yields performance improvements that are very close to the theoretical coding gain limit. With Q = 8 and at BER = 10^{-5}, the coding gain is about 4.5 dB for both convolutional codes considered.

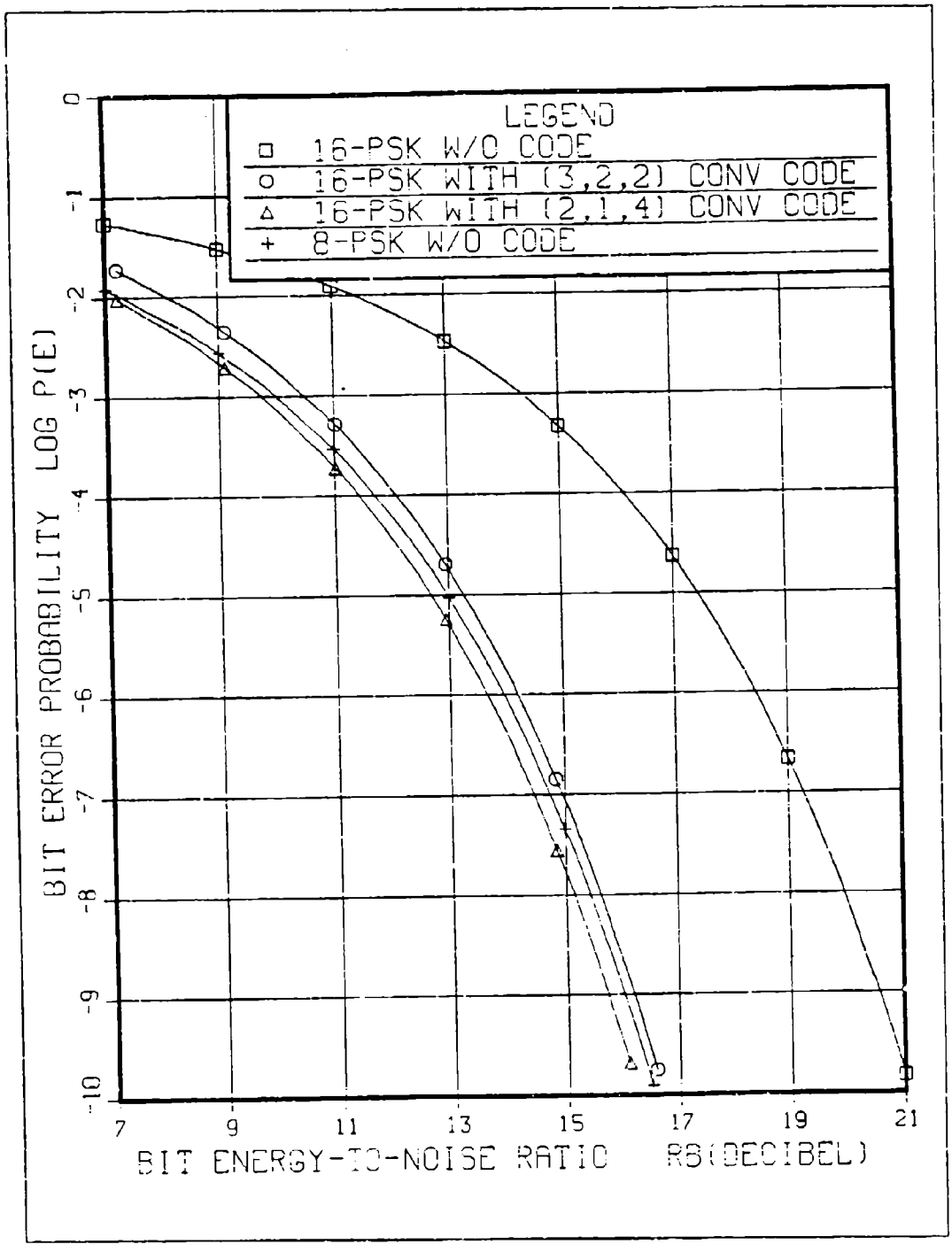

Figure 4.7 Bit error rates of 16-PSK with and without convolutional codes Q = 8

V. CONCLUSIONS

In this thesis, a method to compute the exact bit error rate (BER) for the reception of coherent M-ary PSK signals with Gray code bit mapping and transmitted over an additive white Gaussian noise (AWGN) channel is described. Computation of bit error rates for QPSK, 8-PSK, and 16-PSK modulations were made using the proposed method. The results are summarized in Figure 2.8 where it is shown that the bit error rate performance deteriorates with higher order M-ary modulations. At BER = 10^{-5} or less, the performance loss in signal-to-noise ratio (SNR) is about 3.5 dB between QPSK and 8-PSK and about 4.5 dB between 8-PSK and 16-PSK. Just prior to finishing the writing of this thesis, a published paper [Ref. 9] describing a method for the computation of bit error rates for M-ary PSK signal similar to what was described in this thesis was discovered. While the work were carried out completely independently, the numerical results given in [Ref. 9] and those obtained in this thesis were found to be in extremely close agreement.

Since digital communication techniques are being widely used and higher data rates are constantly being demanded, demodulators that can efficiently operate at high data rates were investigated in the second part of this thesis. The demodulator has to be adaptable to digital implementation in order to take advantage of the VLSI technology, its structure has to be simple and it must allow for parallel bit decoding in order to be able to operate at high data rates. The demodulator must also provide good BER performance in comparison to that of the conventional symbol (followed by bit regeneration) detector. Receiver structures for 8-PSK and 16-PSK were proposed which have certain very desirable features. They allow direct bit detection thus eliminating

the intermediate step of symbol detection followed by mapping the detected symbol into its representative bits. They perform simple arithmetic operation like multiply and subtract. Also binary decisions using zero valued thresholds rather than M-ary decisions need to be implemented. All these along with the parallel decoding of bits provide an attractive scheme for digital implementation and allowing the receiver to operate at high data rates.

The receiver structure for 8-PSK modulation proposed by Thompson [Ref. 3] was analyzed in order to determine its bit error probability. It was found that at BER = 10^{-5}, the performance of this detector was about 3.6 dB inferior to that obtained using a standard 8-PSK phase detection receiver. Modification were made on the receiver structure proposed by Thompson and also extended to the case of 16-PSK modulation. The modified receivers have the desirable features of requiring only zero valued thresholds which are signal energy independent thus eliminating the need for automatic gain control (AGC) circuitry. Most importantly however, the theoretical BER performance of the modified receivers is similar to that obtainable with standard phase detection receivers. However, all the analytical results were carried out on the assumption of the availability of a phase and frequency coherent reference signal. This requires the use an additional phase locked loop (PLL) circuit in order to generate this coherent reference. In a standard phase detection receiver, a differential phase encoding technique is often used in order to allow for a possible phase ambiguity in the coherent reference signal which results in only a slight loss in performance. The differential encoding technique assumes that the unknown phase error of the reference signal remains constant over two symbol intervals so that it can be subtracted away. This method, however, does not appear to be applicable to direct bit

detection methods described in this thesis so that other approaches must be used. A possible solution to this problem involves allocating a portion of the total transmitted power to a residual carrier in order to provide the phase information at the receiver. Modified direct bit detection methods that use table look-up techniques appear to be better solutions to the problem as they are easier to implement and make more efficient use of the transmitter power. At the moment of writing this thesis, the differential encoding method used in conjunction with direct bit detection remains an unresolved issue and the author is unaware of any solution to this problem cited in the literature. The search for a feasible differential encoding scheme that solves this problem should be an interesting and worthwhile topic to be pursued.

The third part of this thesis was devoted to analyzing coding gains obtainable with the use of forward error correction techniques used in conjunction with the modulation techniques described earlier. The methodology developed for obtaining BER's (rather than symbol error rates) was used in order to determine decoded BER's and true coding gains. For the higher order M-ary PSK modulated signals ($M \geq 8$), the signal-to-noise ratio tends to be low so that it is often desirable to improve the BER performance using channel coding. The performance of some simple block and convolutional codes applied to transmission via 16-PSK modulated signals were analyzed and compared along with the uncoded case. Comparisons were also made with transmission using an uncoded 8-PSK modulated signals. It was found that at E_b/N_o = 9 dB, the reduction in BER is in the order 10^2 for coded transmission using a (7,4) Hamming code versus uncoded transmission using 16-PSK modulated signals. The BER reduction obtained from using uncoded 8-PSK modulation versus uncoded 16-PSK modulation was only in the order of

10. This illustrates the superiority of channel coding when operating under weak signal-to-noise conditions. At a BER = 10^{-5}, the coding gain from using the (7,4) Hamming code on 16-PSK modulation is about 4.5 dB. The same coding gain at BER = 10^{-5} can be obtained by using a (3,2,2) or a (2,1,4) convolutional code with Viterbi decoding and soft decisions using levels of output quantization, i.e. Q = 8. At low signal-to-noise ratio, the (7,4) Hamming code is capable of achieving higher coding gains than comparable convolutional codes. This advantage is however offset by the fact that block coding schemes are usually more difficult to implement in hardware and may require look-up tables or complicated decoders to perform their error correcting tasks. Convolutional codes are often easier to implement requiring simple operations like add, compare, and select, which mades them particularly suitable for high speed digital implementation.

LIST OF REFERENCES

1. Lindsey, W.C., and M.K. Simon, *Telecommunications System Engineering*, Prentice Hall, Englewood Cliffs, New Jersey, 1973.

2. Ziemer, R.E., and R.L. Peterson, *Digital Communications and Spread Spectrum Systems*, Macmillan, New York, 1985.

3. Thompson, G.E., *Experimental Evaluation of a New Form of M-ary Phase-Shift-Keying Modulation including Design of Transmitter and Receiver*, Master of Science Thesis, Naval Postgraduate School, December 1984.

4. Proakis, J.G., *Digital Communications*, McGraw-Hill Book Company, 1983.

5. Lin, S., and D.J. Costello, *Error Control Coding: Fundamentals and Applications*, Prentice-Hall, Englewood Cliffs, New Jersey, 1983.

6. Feher, K., *Digital Communications: Satellite/Earth Station Engineering*, Prentice-Hall, Englewood Cliffs, New Jersey, 1983.

7. Heller, J.A., and I.M. Jacobs, *Viterbi Decoding for Satellite and Space Communication*, IEEE Transactions on Communication Technology, October 1971.

8. Wozencraft, J.M., and I.M., Jacobs, *Principles of Communication Engineering*, John Wiley, New York, 1965.

9. Lee, P.J., *Computation of the Bit Error Rate of Coherent M-ary PSK with Gray Code Bit Mapping*, IEEE Transactions on Communications, Vol. COM-34, No. 5, p. 488-491, May 1986.

BIBLIOGRAPHY

Hamming, R.W., *Coding and Information Theory*, Prentice-Hall, Englewood Cliffs, New Jersey, 2nd edition, 1986.

Helstrom, C.W., *Probability and Stochastic Processes for Engineers*, Macmillan, New York, 1984.

Van Trees, H.L., *Detection, Estimation, and Modulation Theory, Volume I*, Wiley, New York, 1968.

Whalen, A.D., *Detection of Signals in Noise*, Academic Press, 1971.

INITIAL DISTRIBUTION LIST

No.		Copies
1.	Defense Technical Information Center Cameron Station Alexandria, Virginia 22304-6145	2
2.	Library, Code 0142 Naval Postgraduate School Monterey, California 93943-5000	2
3.	Department Chairman, Code 62 Department of Electrical and Computer Engineering Naval Postgraduate School Monterey, California 93943-5000	1
4.	Professor Daniel Bukofzer, Code 62Bh Department of Electrical and Computer Engineering Naval Postgraduate School Monterey, California 93943-5000	5
5.	Professor Jeffrey B. Knorr, Code 62Ko Department of Electrical and Computer Engineering Naval Postgraduate School Monterey, California 93943-5000	1
6.	Ministry of Defence Defence Material Organization Paya Lebar Airport Singapore 1953	1
7.	Ministry of Defence Defence Science Organization P.O. Box No. 1050 Ghim Moh Estate Singapore 9127	1
8.	Tan, Chee Seng Defence Material Organization Paya Lebar Airport Singapore 1953	2